

DESIGN AND REDUCTION IN COGGING TORQUE IN RADIAL FLUX PMSBLDC MOTOR

Major Project Report

Submitted in partial fulfillment of the requirements
for the degree of

MASTER OF TECHNOLOGY
IN
ELECTRICAL ENGINEERING
(Power Electronics, Machines and Drives)

By

Amit Kapil

14MEEP01



DEPARTMENT OF ELECTRICAL ENGINEERING
INSTITUTE OF TECHNOLOGY
NIRMA UNIVERSITY
AHMEDABAD-382481

MAY 2016

Certificate

This is to certify that the Major Project entitled "Design and Reduction in Cogging Torque in Radial Flux PMBLDC Motor" submitted by Mr. Amit Kapil (14MEEP01) towards the partial fulfilment of the requirements for the award of degree in Master of Technology (Electrical Engineering) in the field of power Electronics, Machines and Drives of Nirma University is the record of work carried out by him under our supervision and guidance. The work submitted has in our opinion reached a level required for being accepted for examination. The results embodied in this major project work to the best of our knowledge have not been submitted to any other university or Institution for award of any degree or diploma.

Institute Guide

Prof. Amit N. Patel,

Department of Electrical Engineering,

Institute of Technology,

Nirma University,

Ahmedabad.

Head of Department

Department of Electrical Engineerinr,

Institute of Technology,

Nirma University,

Ahmedabad.

Director

Institute of Technology,

Nirma University,

Ahmedabad

Undertaking for Originality of the Work

I, **Amit Kapil** Roll No.14MEEP01, give undertaking that the Major Project entitled “**Design and Reduction in Cogging Torque in Radial flux PMBLDC Motor**” submitted by me, towards the partial fulfillment of the requirement for the degree of Master of Technology in Power Electronics, Machines and Drives, Electrical Engineering, under Institute of Technology, Nirma University, Ahmedabad is the original work carried out by me and I give assurance that no attempt of plagiarism has been made. I understand that in event of any similarity found subsequently with any published work or any Dissertation work elsewhere; it will result in severe disciplinary action.

.....

Signature of Student

Date:

Place: Ahmedabad

Endorsed By:

.....

Project Guide

Prof. Amit N.Patel

Department of Electrical Engineering

Institute of Technology

Nirma University

Ahmedabad

Acknowledgments

I offer my sincere gratitude to Prof. Amit N.Patel (Electrical Engineering Department, IT, NU) for his valuable guidance, motivation and encouragement. He has shown keen interest in this dissertation work right from beginning and has been a great motivating factor in outlining the flow of my work. I am also thankful to my classmates and all the member of Electrical Engineering Department who have directly or indirectly helped me during the project.I would also like to thank Dr. P.N Tekwani, Director, Institute of Technology, Nirma University for allowing me to carry out my project work in house. I am thankful to Nirma University for providing all kind of required resources.

Amit Kapil

14MEEP01

Abstract

Permanent magnet motor offers distinct advantages over conventional electrical motors like high efficiency, compactness, better dynamic response and high speed range. It is always desirable to enhance performance of Permanent Magnet motor. According to direction of flux permanent magnet brushless D.C. motor are classified in two categories 1) radial flux permanent magnet BLDC motor 2) axial flux permanent magnet BLDC motor. Design of radial flux PMSM motor is intensive process as many design variable and constraints are involved. This project is focused on to design and analysis of radial flux PMSM motor. Radial flux permanent magnet brushless D.C Motor suffers from high cogging torque. It is very essential to reduce cogging torque to reduce vibration and noise. Standard ratings radial flux permanent magnet brushless DC motors are analyzed by implementing different techniques to reduce cogging torque in order to improve the performance of the motor. Finite Element Analysis (FEA) has been carried out to validate various techniques.

Abbreviations

B_g	Air gap flux density
B_{sy}	Stator yoke flux density
B_{ry}	Rotor yoke flux density
B_t	Stator teeth flux density
P_0	Output power in watt
V_0	Output voltage
RPM	Rated Speed
Nm	Torque (Newton meter)
kNm/m^3	Torque per unit volume
L	Axial length
D_{s0}	Stator outer Diameter
D_{-r0}	Rotor outer Diameter
η	efficiency
ϕ_g^2	Air gap flux.
R	Air gap reluctance
Θ	Position of Rotor
K_{trv}	Torque per unit rotor volume constant
T	Torque
B_g	Air-gap flux density
Rpm	rotation per minute
η	Efficiency
B_r	Residual flux density
B_{sy}	Stator yoke flux density
B_{ry}	Rotor yoke flux density
B_t	Stator teeth flux density

Nomenclature

PMBLDC	Permanent magnet brushless direct current
PMs	Permanent magnets
Alnico	Aluminium nickel cobalt
EMI	Electro magnetic intereference
Sm-Co	Samarium cobalt
PWM	Pulse width modulation
Nd-Fe-B	Neodymium iron boron
IEEE	Institute of electronic and electrical engineering
CAD	Computer aided design
FEA	Finite element analysis
RFPMBLDC	Radial flux permanent magnet brushless direct current
RPM	Revolution per minute
N	North
S	South

Contents

Certificate	ii
Undertaking for Originality of the Work	iii
Acknowledgments	iv
Abstract	v
Abbreviations	vi
Nomenclatures	vii
List of Tables	x
List of Figures	xii
1 Introduction of PMBLDC Motor	1
1.1 Types of Permanent Magnet Brushless DC Motors	2
1.1.1 Radial Flux Permanent Magnet Brushless DC Motor	3
1.1.2 Axial Flux Permanent Magnet Brushless DC Motor	5
1.2 Features of Radial Flux Permanent Magnet Brushless DC Motor . . .	6
1.3 Operation of PMBLDC Motor	8
1.4 Literature Survey	9
2 PMBLDC Motor Design and Analysis	12
2.1 Main dimension	12
2.2 Stator Model	17
2.3 Rotor Model	18
2.4 Winding Model	19
2.5 Analysis of model	20
2.5.1 Instantaneous Field Analysis	20
2.5.2 Torque Ripple	20
2.5.3 cogging Torque Analysis	21
2.6 Comparison of CAD and FE model	21

3	Cogging Torque Reduction	23
3.1	Cogging Torque Reduction Technique	24
3.1.1	Tooth Tang Radius Technique	24
3.1.2	Magnet Segmentation	28
3.1.3	Magnet edge inset	31
3.1.4	Magnet Retaining sleeve	36
3.1.5	Stator Slot Depth	41
3.1.6	Hiperco 50A material	47
4	Conclusion and Future work	52
4.1	Conclusion	52
4.2	Future work	52
	References	53
A	Introduction to Motor solve	55
B	List of Publication	58

List of Tables

I	K_{trv} value for different type PMBLDC motors	14
II	M 19 material	15
III	Copper	15
IV	Comparison between different magnetic material	16
V	Instantaneous Field Analysis PMBLDC motor	20
VI	Torque ripple Analysis of PMBLDC motor	21
VII	Cogging torque analysis of PMBLDC motor	21
VIII	Comparison of 70 W, 24 V, 350 rpm design of radial flux motor design	21
IX	Comparison of 200 W, 24 V, 1000 rpm design of radial flux motor design	22
X	Comparison of 2.2 kW, 230 V, 1450 rpm design of radial flux motor design	22
XI	Comparison of 20 kW, 230 V, 1500 rpm design of radial flux motor design	22
I	Cogging torque reduction by varying tooth tang radius in 10 kW motor	25
II	Cogging torque reduction by varying tooth tang tang radius in 20 kW motor	26
III	Reduction in cogging torque from initial to improved design by magnet segmentation in 100 W motor	28
IV	Reduction in cogging torque from initial to improved design by magnet segmentation in 70 W motor	30
V	Reduction in cogging torque by varying magnet edge inset in 70 W motor	32
VI	Reduction in cogging torque by varying magnet edge inset in 2.2kW motor	33
VII	Reduction in cogging torque by varying magnet edge inset in 20 kW motor	35
VIII	Cogging torque reduction by varying magnet sleeve in 70 W motor . .	37
IX	Cogging torque reduction by varying magnet sleeve in 2.2 kW motor .	39
X	Cogging torque reduction by varying magnet sleeve in 20 kW motor .	40
XI	Cogging torque reduction by varying stator slot depth in 70 W motor	42
XII	Cogging torque reduction by varying stator slot depth in 2.2 kW motor	44
XIII	Reduction in cogging torque from initial to improved design in 20 kW motor	45

XIV	Reduction in cogging torque by changing stator and rotor material to hiperco 50A material in 70 W motor	48
XV	Reduction in cogging torque by changing stator and rotor material to hiperco 50A material in 2.2 kW motor	49
XVI	Reduction in cogging torque by changing stator and rotor material to hiperco 50A material in 20 kW motor	50

List of Figures

1.1	(a) Interior type rotor PMSM motor design (b) Exterior type rotor PMSM motor design	3
1.2	Interior type magnet	4
1.3	Surface mounted magnet	5
1.4	Axial flux PMSM motor	6
1.5	Operation of PMSM Motor Completing One Complete Cycle in Clockwise direction By exciting Phases in Sequence as shown from A to F	8
2.1	Flow chart of design procedure	13
2.2	Stator of Radial flux motor	17
2.3	Rotor of Radial flux motor Model	18
2.4	Winding model of Radial flux motor Model	19
3.1	Tooth tang radius viewed model	24
3.2	Cogging torque profile of 10 kW motor	25
3.3	10 kW motor Instantaneous field plot of 1.3 mm tooth tang radius . .	26
3.4	Cogging torque profile of 20 kW motor	27
3.5	20 kW motor instantaneous field plot of 6.3 mm tooth tang radius . .	27
3.6	Segmented view of permanent magnet brushless DC motor	28
3.7	Cogging torque profile of 100 W motor	29
3.8	Instantaneous field plot of 100 W motor segmented each magnet into 4 parts	29
3.9	Cogging torque profile of 70 W motor	30
3.10	Instantaneous field plot of 70 W motor segmented each magnet into 4 parts	31
3.11	Design view of magnet edge inset	31
3.12	Cogging Torque plot for 70 W motor	32
3.13	Instantaneous field plot of 70 W motor for 1.5 mm magnet edge inset	33
3.14	Cogging Torque plot for 2.2 kW motor	34
3.15	Instantaneous field plot of 2.2 kW motor for 1.5 mm magnet edge inset	34
3.16	Cogging Torque plot for 20 kW motor	35
3.17	Instantaneous field plot of 20 kW motor for 1.5 mm magnet edge inset	36
3.18	PMSM motor having 0.3 mm magnet sleeve	37

3.19	Cogging torque profile for 70 W motor	38
3.20	Instantaneous field plot of 70 W motor with 0.3 mm magnet sleeve thickness	38
3.21	Cogging torque plot for 2.2 kW motor	39
3.22	Instantaneous field plot of 2.2 kW motor with 0.3 mm magnet sleeve thickness	40
3.23	Cogging torque plot for 20 kW motor	41
3.24	Instantaneous field plot of 2.2 kW motor with 0.3 mm magnet sleeve thickness	41
3.25	(a) Initial design (b) Final design after increment in stator slot depth	42
3.26	Cogging Torque Profile of 70 W motor	43
3.27	Instantaneous field plot of 16.2 mm stator slot depth	43
3.28	Cogging Torque Profile of 2.2 kW model	44
3.29	Instantaneous field plot of 16.2 mm stator slot depth	45
3.30	Cogging Torque Profile of 20 kW model	46
3.31	Instantaneous field plot of 26.3 mm stator slot depth	46
3.32	Stator and rotor material changed M 19 29 Ga to Hiperco 50A in radial flux PMBLDC motor	47
3.33	Cogging Torque Profile of 70 W model	48
3.34	Instantaneous field plot of hiperco 50A material of 70 W motor . . .	48
3.35	Cogging Torque Profile of 2.2 kW model	49
3.36	Instantaneous field plot of hiperco 50A material of 2.2 kW motor . .	50
3.37	Cogging Torque Profile of 20 kW motor	51
3.38	Instantaneous field plot of Hiperco 50A material of 20 kW model . . .	51
A.1	Motor solve work flow	57

Chapter 1

Introduction of PMSM Motor

Permanent magnet BLDC motors are brand new option for researchers because of its features like good efficiency, silent operation, compact size, reliability and maintenance free etc. these features promote use of PMSM motors in many applications, it is found that most of the PMSM motor required sensorless control. The operation of PMSM motors requires rotor- position sensing for controlling the winding currents. The Sensorless control would need estimation of rotor position from the voltage and current signals, which are easily sensed. Replacement of electromagnetic magnet in place of electromagnetic excitation results in many advantages such as no excitation losses, simplified construction, improved efficiency, improve performance, and increase torque. From early 19th century permanent magnet motors are first used, but not used widely due to permanent magnet material having poor quality. Invention of Alnico in 1932 revived use of permanent magnet excitation systems, but it is limited to small and fractional horse power dc commutator motors [1]. Due to rugged construction, in 20th century, squirrel cage induction motors is widely adopted. Improvement and advancements in power electronics and digital signal processors improved features of motor drives to make them more use by industries. But poor power factor and efficiency is one of the drawback of the induction motor compared with synchronous motor and On the other hand drawback such as poor speed, noise problems, wear and EMI in synchronous and induction mo-

tor lead to development of PMBLDC motor. Therefore, permanent magnet brushless motors can be considered a kind of three phase synchronous motor, having permanent magnets on the rotor, replacing the mechanical commutator and brush gear. Commutation is achieved by electronic switches, which supply current to the motor windings to synchronize rotor position. Day by day popularity of PMBLDC motors are increasing due to PMBLDC motors are increasing due to high energy density availability and cost effective earth PM materials like Samarium Cobalt (Sm-Co) and Nd-Fe-B which enhance performance of PMBLDC Motor drives and lessen losses and size of motor. Improvement in design and geometry made the use of PMBLDC motor in different area like domestic, commercial and industrial applications. Due to excellent dynamic capability, lessen losses and high torque/weight ratio promote use of PMBLDC motor in position control and medium sized industrial drives. its application are diverse in nature like automobiles, aerospace, power tools, toys, sound equipment, health care, transportation. Advanced control algorithms and ultra-fast processors have made PMBLDC motors suitable for position control in machine tools, robotics and high precision servos, speed control and torque control in various industrial drives and process control applications. Advancement in power electronics make it possible to design PMBLDC generators for power generation onboard ships, aircraft, hybrid electric cars and buses. By reduced generator weight, size and a high payload capacity for the complete vehicles[2].

1.1 Types of Permanent Magnet Brushless DC Motors

- Radial Flux Permanent Magnet Brushless DC Motors
- Axial Flux Permanent Magnet Brushless DC Motors

1.1.1 Radial Flux Permanent Magnet Brushless DC Motor

Radial flux Permanent magnet motor used in various domestic and industrial applications. Permanent magnet on rotor is placed in two configurations[1].

- Interior
- Surface Mounted

Radial flux permanent magnet brushless DC motors is shown in fig 1.1(a) Rotor is placed inside the stator. This structure provides protection to rotor from outer environment. In fig 1.1(b) rotor appears outside the stator. This configuration is called "inside-out" motor. Flux travels in the radial direction and interacts with current flowing in the axial direction.

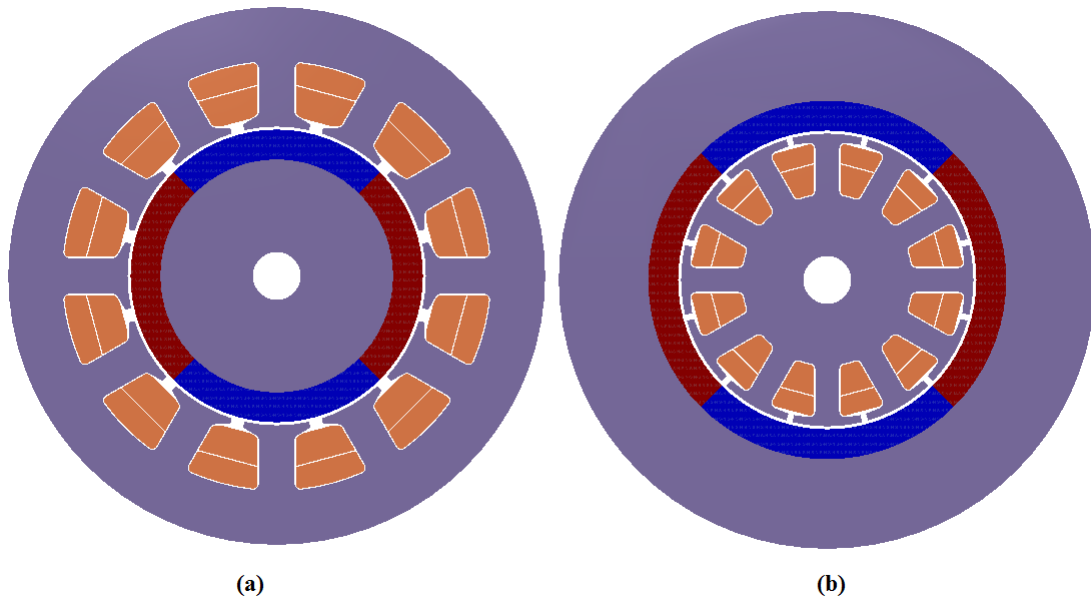


Figure 1.1: (a) Interior type rotor PMBLDC motor design (b) Exterior type rotor PMBLDC motor design

Interior: Here the magnets appear orthogonal to the air gap, rather than facing it, and the magnet flux is directed to the air gap through electrical steel. This

configuration is popular when higher performance is desired when using inexpensive ferrite magnets.[2]

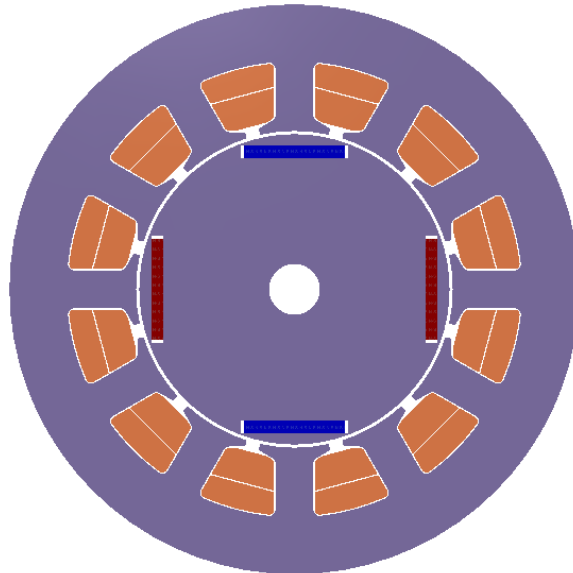


Figure 1.2: Interior type magnet

- Less cogging torque
- Highly robust construction
- Long life span
- Less noise
- More permanent magnet material is required

Surface Mounted : surface mounted permanent magnet rotor configuration. Here the magnets are mounted on the surface of the rotor. It is advisable for lower speed applications.[3]

- Less robust construction
- High cogging torque

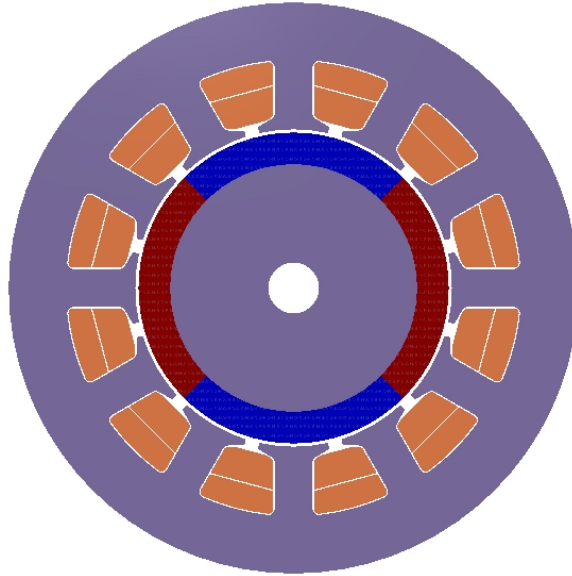


Figure 1.3: Surface mounted magnet

- Long life
- More noise
- Less permanent magnet mass is required
- Less damping

1.1.2 Axial Flux Permanent Magnet Brushless DC Motor

Axial Flux Permanent Magnet Brushless DC Motors found applications, where the motor axial dimension is more limited than the radial dimension. Flux travel in the axial direction and interacts with current flowing in the radial direction [1]. Axial Flux Motors can be constructed in one of the following ways:

- Single stator and single rotor (one air-gap)
- Single stator sandwiched between two rotors (Double air-gap)
- Single rotor sandwiched between two stators (Double air-gap)

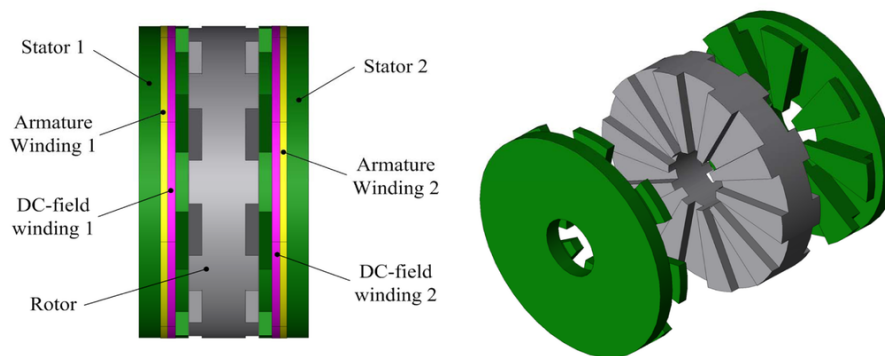


Figure 1.4: Axial flux PMBLDC motor

- Multiple rotors and stators (Multiple air-gap)

Laminations of stack must be in circumferential direction, which makes the fabrication of axial flux PMBLDC motor more complicated compare to radial flux PMBLDC motor. Also the weight of motor is more. The air gap is adjustable during and after assembly which is not possible in case of RFPMBLDC motors. Rotor permanent magnet material requirement is also more.

1.2 Features of Radial Flux Permanent Magnet Brushless DC Motor

Rotor of BLDC motor is mainly made out of permanent magnets. According to application demand number of rotor pole is vary. it is found that by variation in pole improve torque but on other hand affect the maximum possible speed.[1][2]

Advantages

- Improved Efficiency
- Higher Torque capability

- High torque to inertia ratio
- Higher power density
- Higher torque per ampere ratio
- Less noise

Disadvantages

- Costly
- Closed loop control is must
- Cogging torque

Application

- Computer peripheral
- Aerospace
- Defence equipment
- Medical
- Instrumentation
- Marine

1.3 Operation of PMSM Motor

[1] Internal shaft position feedback is working principle of a PMSM motor. In brushed DC motor feedback is implemented by using mechanical commutator and brushes. In PMSM motor done by help of multiple feedback sensors.

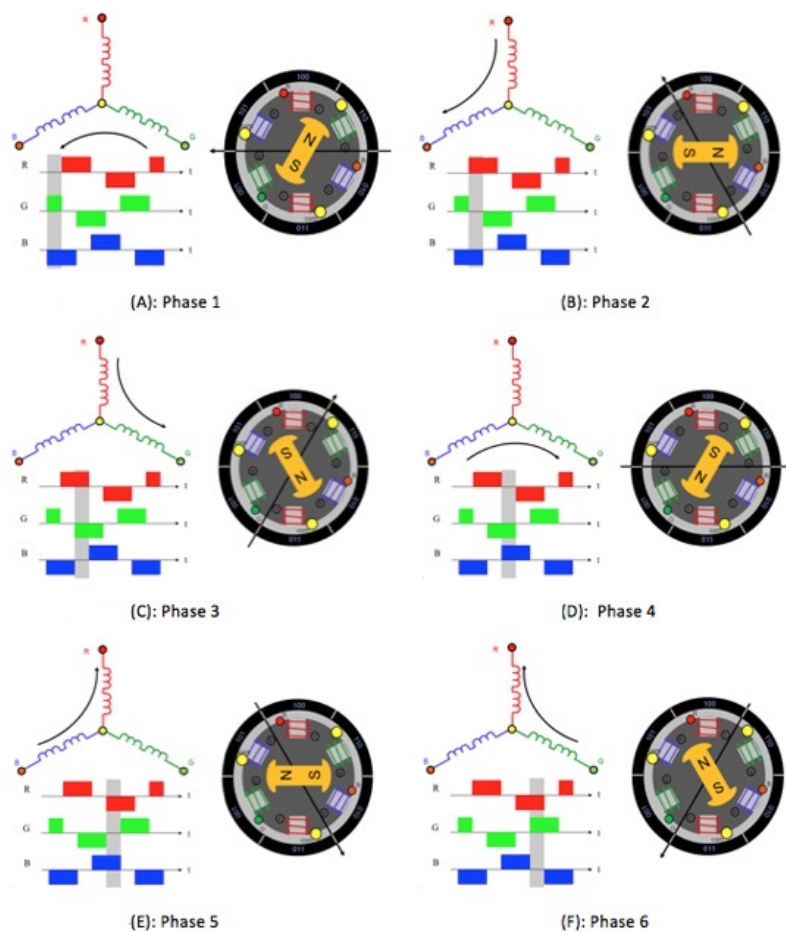


Figure 1.5: Operation of PMSM Motor Completing One Complete Cycle in Clockwise direction By exciting Phases in Sequence as shown from A to F

Hall sensors and optical encoders are frequently used sensors. It is to be noted that hall sensors work on principle of hall effect principle, it says that when current-carrying conductor is disclosed to the magnetic field, charge carriers experience a

force based on the voltage developed across the two sides of the conductor. If the direction of the magnetic field is reversed, voltage developed will reverse as well. For Hall-effect sensors used in PMBLDC motors, whenever rotor magnetic poles (N or S) pass near the hall sensor, they generate a high or low level signal, which can be used to identify the position of the shaft. As shown in figure 4 (A), the GREEN winding labeled 001 is energized as the NORTH pole and the BLUE winding labeled as 010 is energized as the SOUTH pole. Because of this excitation, the SOUTH pole of the rotor aligns with the GREEN winding and the NORTH pole aligns with the RED winding labeled 100. In order to move the rotor, the RED and BLUE windings are energized in the direction shown in figure 4 (B). This causes the RED winding to become the NORTH pole and the BLUE winding to become the south pole. This shifting of the magnetic field in the stator produces torque because of the development of repulsion (red winding north-north alignment) and attraction forces (blue winding north-south alignment), which moves the rotor in the clockwise direction.[?]

1.4 Literature Survey

Permanent magnet BLDC motors are brand new option for researchers because of its features like good efficiency, silent operation, compact size, reliability and maintenance free etc. these features promote use of PMBLDC motors in many applications. The operation of PMBLDC motors requires rotor- position sensing for controlling the winding currents [1].

Invention of Alnico in 1932 revived use of permanent magnet excitation systems, but it is limited to small and fractional horse power dc commutator motors. PM materials like Samarium Cobalt (Sm-Co) and Nd-Fe-B which enhance performance of PMBLDC Motor drives and lessen losses and size of motor. Improvement in design and geometry made the use of PMBLDC motor in different area like domestic, commercial and industrial applications [2].

Analyzed three different rating motors flux density plot which is maximum in teeth and minimum in stator and rotor yoke. It is found that 1.9 T is maximum flux density range for M 19 and CR 10 motor material above 1.9 T motor goes into saturation region and similarly for 2.2 T for Hiperco 50A material [3].

Explanation and derivation to cogging torque by differentiating magnetic field energy with respect to mechanical angle[4].

Cogging torque calculation is done by using virtual calculation method and different methods are proposed to reduce cogging torque which are **Air Gap Length** : The distance between rotor and stator refers to air-gap length which is varied for all the standard rating motors respectively 0.12-0.25mm in small rating, 0.38- 0.5mm in medium rating and 0.63-0.88mm in high rating motors. some techniques are applied to reduce cogging torque are Magnet pole shaping, Skewing, Lowering magnet flux density,addition of dummy slot, slot opening [5].

However, when increasing air-gap length, its reluctance is increased. As a result, air gap flux is finally lowered cogging torque [6] .

Concept increasing of air-gap length of lowering magnetic flux density techniques are , increasing number of slots/pole, thickness of proper magnet tip techniques,magnet shape, mounting of magnet and slot skewing are used and reduced cogging torque in all the standard ratings motors[6].

The design variables such as air-gap flux density and torque per unit rotor volume are assumed.It is clear that as $K_t r v$ increases, main dimensions of motor will decrease and copper loss will increase. The basic output equations are derived and used for the CAD program. The developed CAD program gives dimensions and performance of the motor. Two different motors of rating 10 kW and 5 kW are designed using the developed program and then compared with Motor Solve result to validate the design.[8]

70 W, 350 rpm, axial-field and radial-field permanent magnet brushless dc motors is compared using computer aided design CAD and finite element FE methods. The design variables like number of poles, slots per pole per phase, airgap length, airgap flux density, slot electric loading, stator flux density, and the permanent magnet material are changed one at a time and the performances are calculated using the developed CAD program. It is observed that the axial-field motor gives higher efficiency, whereas the radial-field motor has less weight.[9]

comparative study has shown that the eddy current loss in the stainless steel sleeve is much higher than that in the carbon fiber sleeve, while, the eddy current loss in magnets of the motor with stainless sleeve is lower than that with carbon-fiber sleeve. In result, the overall rotor eddy current loss of the motor with carbon-fiber sleeve is higher than that with stainless sleeve.it mean that carbon-fiber sleeve is superior in reducing rotor current loss[10].

Losses in the Titanium sleeve is much higher than that in the carbon fiber sleeve. However, the eddy current in the Titanium sleeve smooths the field in the magnets, hence, reduces the loss in the magnets. In result, the overall rotor loss is similar for both sleeve materials. Furthermore, the influence of the copper shield between the retaining sleeve and magnets is inspected. Although eddy-current loss occurs in the shield, the losses in the other rotor parts are dramatically reduced, resulting in a much lower overall rotor loss. Moreover, there is no locally overheated area in the rotor, and the rotor temperature drops significantly by utilizing the copper shield[11].

Most superior property of hiperco 50 and hiperco 50A having high flux density that is 2.2 T to get saturate[12].

Chapter 2

PMBLDC Motor Design and Analysis

Four main steps for design of Radial Flux Permanent Magnet Brushless DC motor are:

- Main Dimension
- Stator Design
- Rotor Design
- Performance Estimation

2.1 Main dimension

D_{so} = Stator outer diameter

D_{ro} = Rotor outer diameter

L = Axial length

These main dimensions are calculated based on assumption of various design variables, such as K_{trv} , split ratio and aspect ratio.

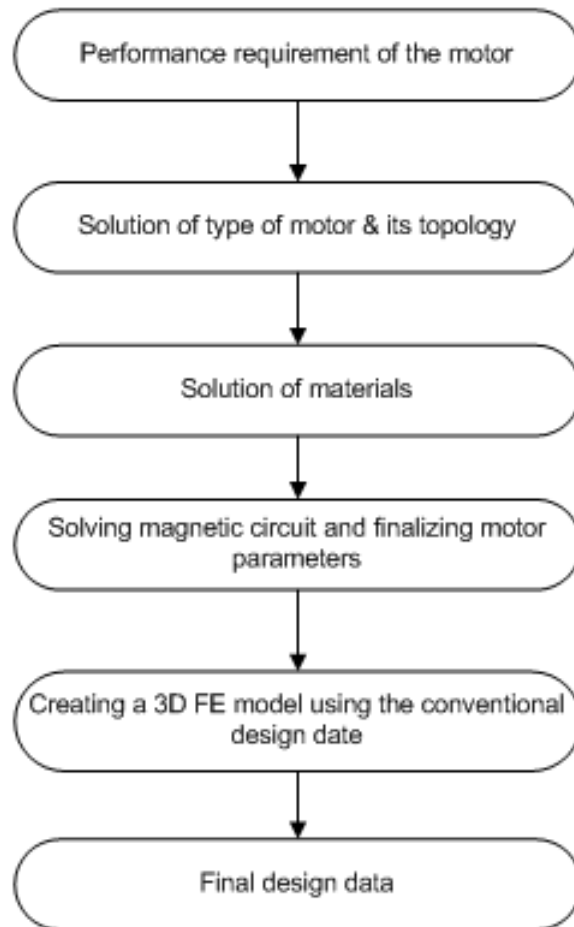


Figure 2.1: Flow chart of design procedure

Torque per unit volume (k_{trv})

It is defined as torque per unit volume. Range for K_{trv} is given below. For the fixed rotor outer diameter, torque per unit volume is directly proportional to the air gap flux-density B_g , the number of magnet poles N_m and the coil ampere - turns. As the volume of the motor increases the torque per unit volume decreases.

Table I: K_{trv} value for different type PMLDC motors

Sr. No	Type of motor	k_{trv} (kNm/m ³)
1	Totally enclosed motor ; 1 kW motors	1.4 - 4
2	Totally enclosed motor (ferrite)	7 - 14
3	Totally enclosed motor (Ndfeb)	14 - 42
4	High performance motors	15 - 50
5	Aerospace motors	30 - 75

Aspect Ratio:

Aspect ratio is defined as the ratio of axial length to the stator outer diameter.
formula of aspect ratio is :

$$Aspectratio = \frac{L}{D_{so}} \quad (2.1)$$

Split Ratio:

Split ratio is defined as the ratio of rotor outer diameter to the stator outer diameter.
formula of split ratio is:

$$Splitratio = \frac{D_{ro}}{D_{so}} \quad (2.2)$$

Calculation of Main Dimension :

Main dimensions like rotor outer diameter, stator outer diameter and axial length are calculated by given below equation:

$$Splitratio = \frac{D_{ro}}{D_{so}} \quad (2.3)$$

$$D_{so} = \frac{L}{aspectratio} \quad (2.4)$$

$$D_{ro} = D_{so} \quad X \quad \text{splitratio} \quad (2.5)$$

Selection of material

Table II: M 19 material

Material	Non oriented silicon steel (M 19)
Iron loss	3.17 (W/Kg)
Thermal conductivity	3.17 (W/mC)
Mass density	7650 (W/mC)

Selection of material plays very significant role on the performance of PMBLDC motor. M 19 is probably the most common grade for motion control products, as it offers the lowest core loss. In reference to this M-19 29 Ga is the best suitable as rotor and stator core material.

Winding Material

Table III: Copper

Material	Copper
specific heat capacity	393 (J/Kg)
Thermal conductivity	3.17 (W/mC)
Mass density	7650 (kg/m ₃)

Due to the high conductivity and very low resistivity, copper is best suitable for winding material. Winding losses are very less and as a result generation of heat is very less.

Permanent Magnet Material

Among the available permanent magnet materials, Alnico magnets can have flux densities equivalent to soft magnetic irons but due to lower values of coercive force it get demagnetized easily. Ceramic magnets are economical but their maximum energy density product is low due to the lower values of retentivity. Rare earth and samarium cobalt alloys have relatively good magnetic properties, but cost of these material is very high. A neodymium magnet is the most widely used rare earth magnet made from an alloy of neodymium,iron and boron to form the $Nd_2Fe_{14}B$, tetragonal structure. It gives the potential to have high coercivity, high saturation magnetization.

Some common terms to determine Magnetic Properties are :

Remanence (B_r) : It measures the strength of the magnetic field.

Coercivity H_c : It specifies the material's resistance to get demagnetized.

Curie temperature (T_c) : It is the temperature at which the material loses its magnetic property.

Neodymium magnets have higher remanence and coercivity, but lower curie temperature than other types of permanent magnet material. Neodymium is alloyed with terbium and dysprosium in order to preserve its magnetic properties at high temperatures.

Different Permanent Magnetic Material Properties

Table IV: Comparison between different magnetic material

Magnets	Residual flux density (B_r)	Coercivity (H_c)	curie temperature (c)
$Nd_2Fe_{14}B$	1.0 - 1.4	750 - 2000	310
$SmCo_5$	0.8 - 1.1	600 - 2000	720
Alnico	0.6 - 1.4	275	700

2.2 Stator Model

on the basis of required rating radial flux PMBLDC motor has been modeled. Stator model required different parameters like inner diameter in mm, outer diameter in mm, back-iron depth in mm, shank length in mm, slot area in mm², slot depth in mm, tooth gap width in mm, tooth width in mm.

Detail of Stator model

- stator backiron material
- stator coil type
- stator coil material

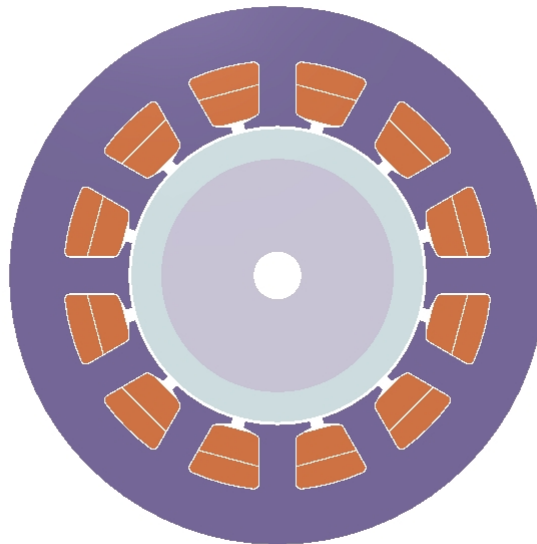


Figure 2.2: Stator of Radial flux motor

2.3 Rotor Model

on the basis of required rating radial flux PMBLDC motor has been modeled. Rotor model required parameters like inner diameter in mm, outer diameter in mm, stator back-iron in mm, magnet angle in degree, magnet gap angle in degree, magnet thickness in mm.

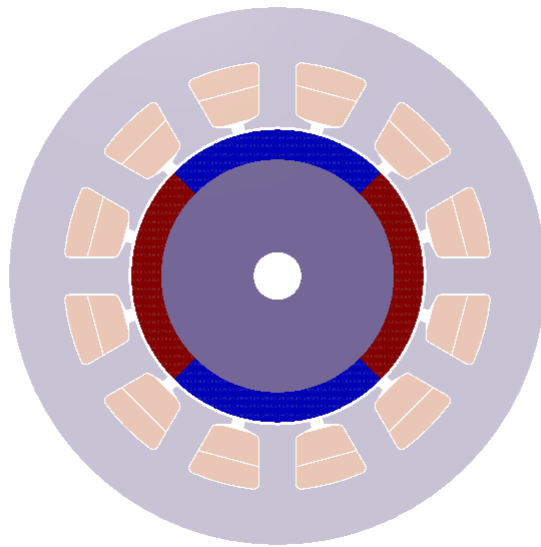


Figure 2.3: Rotor of Radial flux motor Model

Detail of Rotor model

- Rotor type
- Mounting of magnet on rotor i.e exterior or interior
- Rotor core material
- Rotor magnet material

2.4 Winding Model

Stator winding model input data is connection type, number of parallel path, PWM method, current hysteresis, coil placement method, wire size method, SWG number,

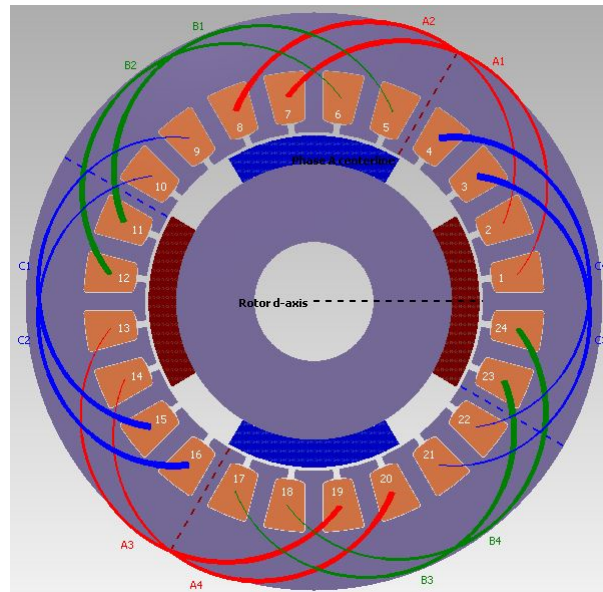


Figure 2.4: Winding model of Radial flux motor Model

winding type, coil span, number of layer, number of turns. The number of stator slot per pole per phase value is 2 and the coil span is 6. So for the R Phase the coil is wound from 1 to 7, 2 to 8, 13 to 19, 14 to 20. and then phase displacement between the R phase and Y phase is 120 electrical degree. Here between two slot phase different is 30 electrical degree. So the Y phase is started from the 5 to 1, 16 to 12, 17 to 23, 18 to 24.

Detail of Winding model

- SWG number
- wire size method

- Connection type
- Coil span

2.5 Analysis of model

2.5.1 Instantaneous Field Analysis

Values of flux density in different magnetic circuit is assumed during the design procedure. These values should be within a tolerable limit to avoid saturation. It is observed that the flux density in different sections of the magnetic circuit is as per the assumptions. If values differ from the assumption, then modification in magnet circuit has to be done. Instantaneous field analysis for 70 W, 200 W, 2200 W, 20000 W Radial Flux PMBLDC motor is shown in figure.

Table V: Instantaneous Field Analysis PMBLDC motor

Sr. No.	Parameter	Values
1	Air gap flux density (B_g)	0.5
2	Stator Yoke flux density (B_{sy})	1.5
3	Rotor Yoke flux density (B_{ry})	1.5
4	Stator teeth flux density (B_t)	1.9

2.5.2 Torque Ripple

It is the relation between rotor position (degree) and torque (Nm). From this profile, torque ripple is found out. Torque profile for 70 W, 200 W, 2200 W, 20000 W Radial Flux PMBLDC motor is shown in figure.

Table VI: Torque ripple Analysis of PMBLDC motor

Sr. No.	Motor Rating	$(T_{max}-T_{min})/T$ (N.m)
1	70 W	1.79
2	200 W	0.43
3	2200 W	0.75
4	20000 W	0.57

2.5.3 cogging Torque Analysis

Cogging torque is generated due to interaction between the magnets of the rotor and the stator teeth. It is an undesirable quantity that affects smooth rotation of the rotor and generates noise and Vibration It is the relation between peak to peak cogging torque (Nm) and rotor position (degree).

Table VII: Cogging torque analysis of PMBLDC motor

Sr. No.	Motor Rating	Peak-Peak N.m
1	70 W	0.536
2	200 W	3.3
3	2200 w	8.84
4	20000	57.2

2.6 Comparison of CAD and FE model

Table VIII: Comparison of 70 W, 24 V, 350 rpm design of radial flux motor design

Parameter	CAD Programming	FE method
Torque (N.m.)	1.9	1.91
Air gap flux density (Bg)	0.5	0.4
Stator Yoke flux density (Bsy)	1.5	1.53
Rotor Yoke flux density (Bry)	1.5	1.5
Stator teeth flux density (Bt)	1.9	1.9
Efficency η (derived) ”%”	85.6	84.7

Table IX: Comparison of 200 W, 24 V, 1000 rpm design of radial flux motor design

Parameter	CAD Programming	FE method
Torque (N.m.)	1.9	1.91
Air gap flux density (Bg)	0.5	0.4
Stator Yoke flux density (Bsy)	1.5	1.6
Rotor Yoke flux density (Bry)	1.5	1.5
Stator teeth flux density (Bt)	1.9	1.9
Efficiency η (Derived) "%"	85.6	85.3

Table X: Comparison of 2.2 kW, 230 V, 1450 rpm design of radial flux motor design

Parameter	CAD Programming	FE method
Torque (N.m.)	14.48	14.5
Air gap flux density (Bg)	0.5	0.6
Stator Yoke flux density (Bsy)	1.5	1.52
Rotor Yoke flux density (Bry)	1.5	1.5
Stator teeth flux density (Bt)	1.9	1.9
Efficiency η (derived) "%"	96.1	84.7

Table XI: Comparison of 20 kW, 230 V, 1500 rpm design of radial flux motor design

Parameter	CAD Programming	FE method
Torque (N.m.)	127.3	127
Air gap flux density (Bg)	0.5	0.48
Stator Yoke flux density (Bsy)	1.5	1.53
Rotor Yoke flux density (Bry)	1.5	1.5
Stator teeth flux density (Bt)	1.9	1.92
Efficiency η (Derived) "%"	97	97

Chapter 3

Cogging Torque Reduction

Although permanent magnet brushless DC motor has several advantages over conventional DC motor, a major drawback of permanent magnet motors are high cogging torque. Permanent magnet brushless DC applications require minimum cogging torque for reducing vibration and noise for smooth operation of the motor. In most of the applications, torque quality becomes exceptional. Motor design and analysis must be analyzed paying attention to cogging torque. There are two torque components that affects the performance of PMBLDC motor.

- Cogging torque
- Ripple torque

Permanent magnet motors have major drawback of high torque ripple that is inherent according to their. This ripple is parasitic, and can prompt mechanical vibration, acoustic noise, and issues in drive systems. Minimizing this ripple is of incredible significance in the configuration of a permanent magnet motors. cogging torque is the prime creator of torque ripple. Cogging torque is defined as interaction between the magnets of the rotor and the stator teeth. It is also known as 'detent' or 'no current' torque.

$$T_{cog} = \frac{-1}{2} \Phi_g^2 \frac{dR}{d\Theta} \quad (3.1)$$

[6]

In the above cogging torque equation Φ_g , R and Θ denotes air gap flux, air gap reluctance and the position of the rotor respectively

3.1 Cogging Torque Reduction Technique

Minimization of cogging torque can be done by forcing either the air-gap flux, Φ_g or the rate of change of the air-gap reluctance, $\frac{dR}{d\Theta}$ to be zero. Since the air-gap flux is needed for the generation of useful torque components that drive the motors therefore it is not possible to make Φ_g to be zero. Therefore, cogging torque can be minimized by forcing the air-gap resistance to be constant with respect to rotor position. Practically speaking, cogging torque cannot be effectively removed, however it can be highly reduced with proper techniques

3.1.1 Tooth Tang Radius Technique

In this technique by increasing tooth tang radius of motor it will reduce the cogging torque. This technique is applicable in higher rating motors. This technique is being tested on 20 kW and 10 kW permanent magnet brushless DC motor.

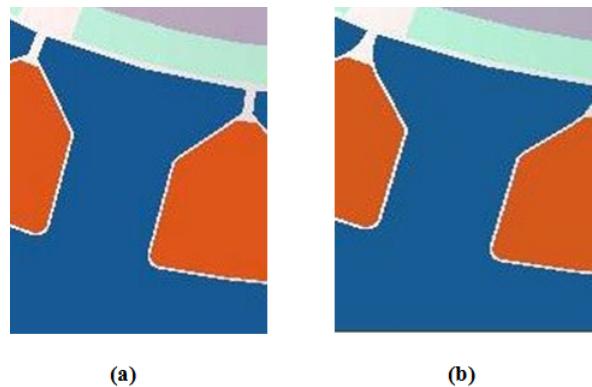


Figure 3.1: Tooth tang radius viewed model

1. 10 kW Radial flux PMBLDC motor

10 kW radial flux permeant magnet brushless DC motor is designed based on sizing equations. Computer aided design algorithm is developed for whole design. Model based on design information is prepared and carry out finite element analysis.

Table I: Cogging torque reduction by varying tooth tang radius in 10 kW motor

Parameters	Initial design mm	Improved design tooth tang radius	
		1 mm	1.3 mm
T cog (N.m.)	29.8	25	21.4
T avg (N.m.)	95.8	96	96

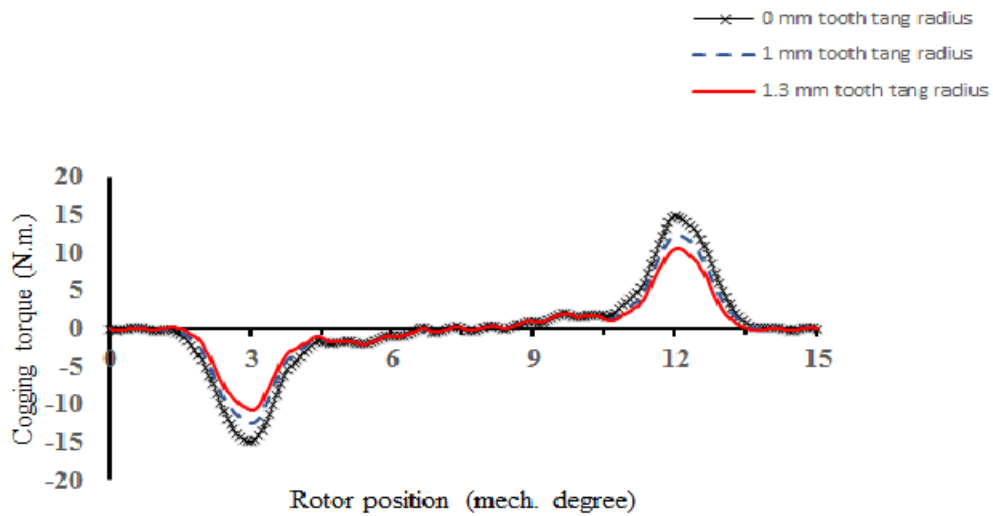


Figure 3.2: Cogging torque profile of 10 kW motor

Tooth tang radius is varied in improved design by maintaining other design parameters same. Finite element analysis is performed to obtain cogging torque profile. Cogging torque profile is influenced and reduced. It is observed that peak to peak cogging torque is reduced without affecting other performance indicators. It is observed that flux density in different section of magnetic circuit

is as per the assumption.

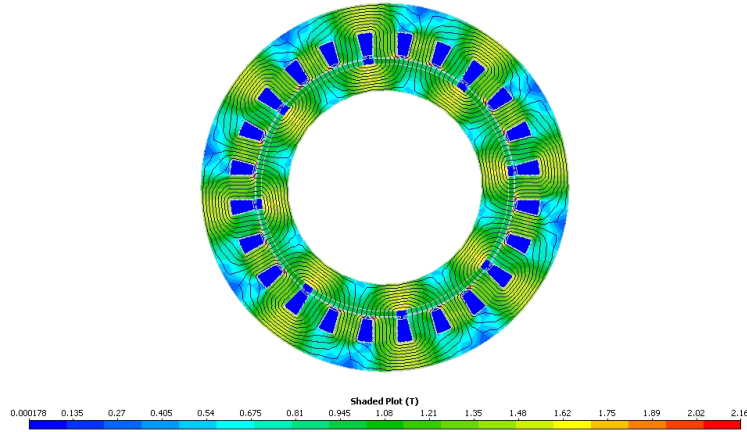


Figure 3.3: 10 kW motor Instantaneous field plot of 1.3 mm tooth tang radius

2. 20 kW Radial flux PMSM motor

20 kW radial flux permanent magnet brushless DC motor is designed based on sizing equations. Computer aided design algorithm is developed for whole design. Model based on design information is prepared and carry out finite element analysis.

Table II: Cogging torque reduction by varying tooth tang radius in 20 kW motor

Parameters	Initial design mm	Improved design tooth tang radius	
		3.15 mm	6.3 mm
T cog (N.m.)	39.2	32.2	24.4
T avg (N.m.)	127	127	127

Tooth tang radius is varied in improved design by maintaining other design parameters same. Finite element analysis is performed to obtain cogging torque profile. Cogging torque profile is influenced and reduced. It is observed that

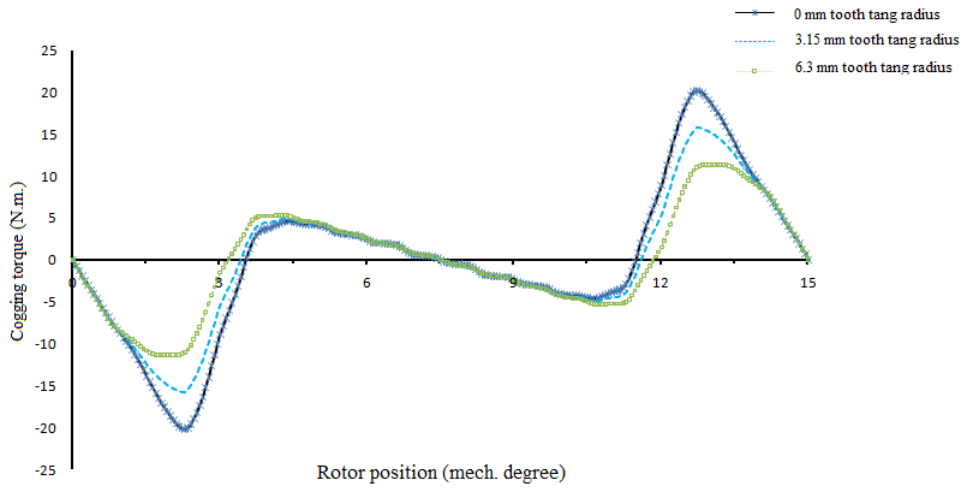


Figure 3.4: Cogging torque profile of 20 kW motor

peak to peak cogging torque is reduced without affecting other performance indicators. It is observed that flux density in different section of magnetic circuit is as per the assumption.

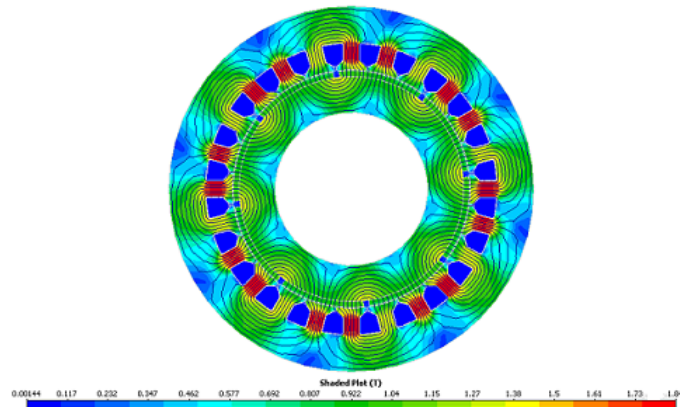


Figure 3.5: 20 kW motor instantaneous field plot of 6.3 mm tooth tang radius

3.1.2 Magnet Segmentation

In this technique of magnet segmentation, magnet is segmented into parts without changing its overall density. By doing magnet segmentation effectively reduced cogging torque in 70 W and 100 W. This method for low rating motors.

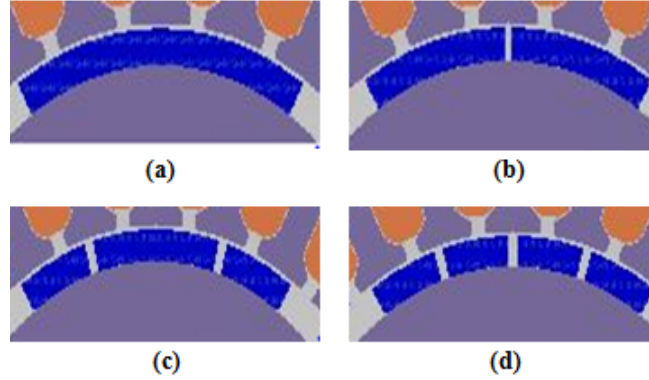


Figure 3.6: Segmented view of permanent magnet brushless DC motor

1. 100 W Radial flux PMBLDC motor

100 W radial flux permanent magnet brushless DC motor is designed based on sizing equations. Computer aided design algorithm is developed for whole design. Model based on design information is prepared and carry out finite element analysis.

Table III: Reduction in cogging torque from initial to improved design by magnet segmentation in 100 W motor

Parameters	Initial design	Improved design Magnet segmentation		
		2	3	4
T_{cog} (N.m.)	1.870	1.56	1.31	0.732
T_{avg} (N. m.)	6.3	5.9	6.2	6.2

Magnet segmentation is varied in improved design by maintaining other design parameters same. Finite element analysis is performed to obtain cogging torque

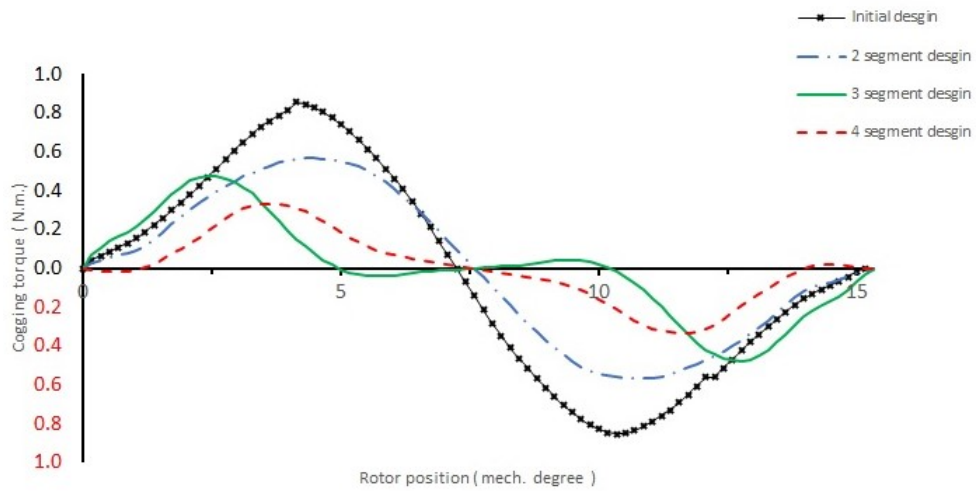


Figure 3.7: Cogging torque profile of 100 W motor

profile. Cogging torque profile is influenced and reduced. It is observed that peak to peak cogging torque is reduced without affecting other performance indicators. It is observed that flux density in different section of magnetic circuit is as per the assumption.

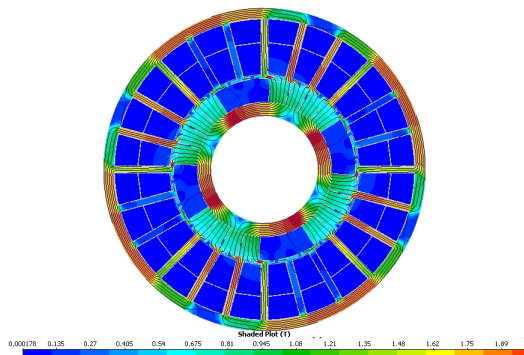


Figure 3.8: Instantaneous field plot of 100 W motor segmented each magnet into 4 parts

2. 70 W Radial flux PMBLDC motor 70 W radial flux PMBLDC motor is designed based on sizing equations. Computer aided design algorithm is

developed for whole design. Model based on design information is prepared and carry out finite element analysis.

Table IV: Reduction in cogging torque from initial to improved design by magnet segmentation in 70 W motor

Parameters	Initial design	Improved design magnet segmentation		
		2	3	4
T cog (N.m.)	0.574	0.418	0.282	0.155
T avg (N. m.)	1.9	1.89	1.89	1.89

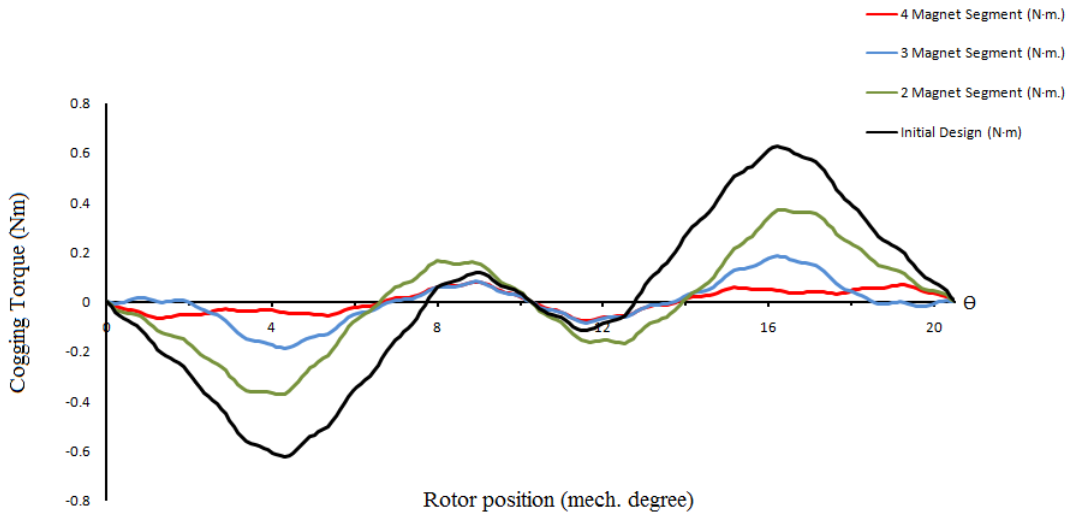


Figure 3.9: Cogging torque profile of 70 W motor

Magnet segmentation is varied in improved design by maintaining other design parameters same. Finite element analysis is performed to obtain cogging torque profile. Cogging torque profile is influenced and reduced. It is observed that peak to peak cogging torque is reduced without affecting other performance indicators. It is observed that flux density in different section of magnetic circuit is as per the assumption.

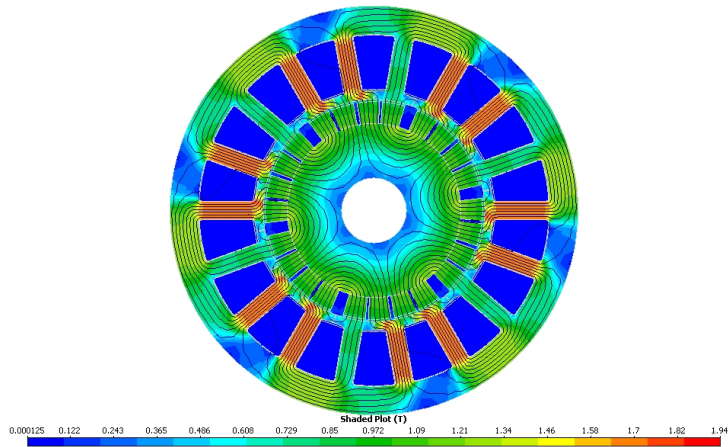


Figure 3.10: Instantaneous field plot of 70 W motor segmented each magnet into 4 parts

3.1.3 Magnet edge inset

In this technique cogging torque is gets reduced by increasing skewing edge inset of magnet from 0 mm to 1.5 mm and found minimum cogging torque at 1.5 mm . This technique is applicable in all standard rating of motor. This technique is being tested on 70 W, 2.2 kW and 20 kW motor.

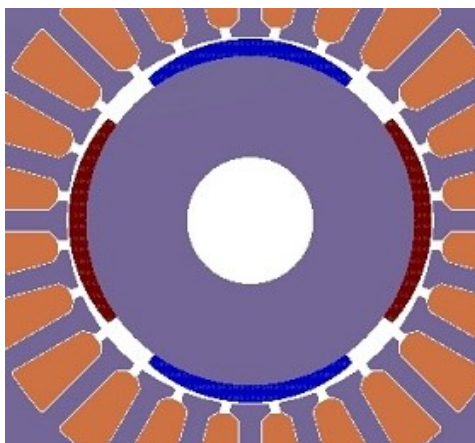


Figure 3.11: Design view of magnet edge inset

1. 70 W Radial flux PMBLDC motor

70 W radial flux PMBLDC motor is designed based on sizing equations. Computer aided design algorithm is developed for whole design. Model based on design information is prepared and carry out finite element analysis.

Table V: Reduction in cogging torque by varying magnet edge inset in 70 W motor

Parameters	Initial design mm	Improved design magnet edge inset in mm		
		0.5	1	1.5
T cog (N.m.)	0.1886	0.0754	0.032	0.0129
T avg (N. m.)	1.91	1.9	1.91	1.9

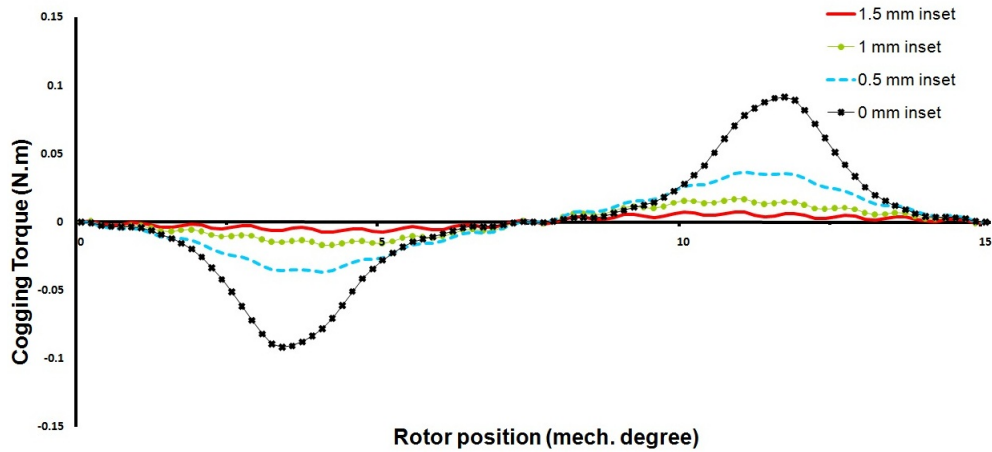


Figure 3.12: Cogging Torque plot for 70 W motor

Magnet edge inset is varied in improved design by maintaining other design parameters same. Finite element analysis is performed to obtain cogging torque profile. Cogging torque profile is influenced and reduced. It is observed that peak to peak cogging torque is reduced without affecting other performance indicators. It is observed that flux density in different section of magnetic circuit is as per the assumption.

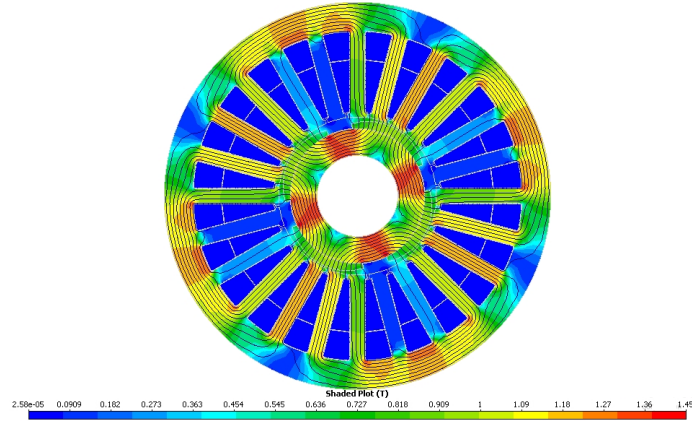


Figure 3.13: Instantaneous field plot of 70 W motor for 1.5 mm magnet edge inset

2. 2.2 kW Radial flux PMLDC motor

2.2 kW radial flux permanent magnet brushless DC motor is designed based on sizing equations. Computer aided design algorithm is developed for whole design. Model based on design information is prepared and carry out finite element analysis.

Table VI: Reduction in cogging torque by varying magnet edge inset in 2.2kW motor

Parameters	Initial design mm	Improved design magnet inset in mm		
		0.5	1	1.5
T cog (N.m.)	2.02	1.18	0.628	0.302
T avg (N. m.)	14.4	14.4	14.5	14.5

Magnet edge inset is varied in improved design by maintaining other design parameters same. Finite element analysis is performed to obtain cogging torque profile. Cogging torque profile is influenced and reduced. It is observed that peak to peak cogging torque is reduced without affecting other performance indicators. It is observed that flux density in different section of magnetic circuit is as per the assumption.

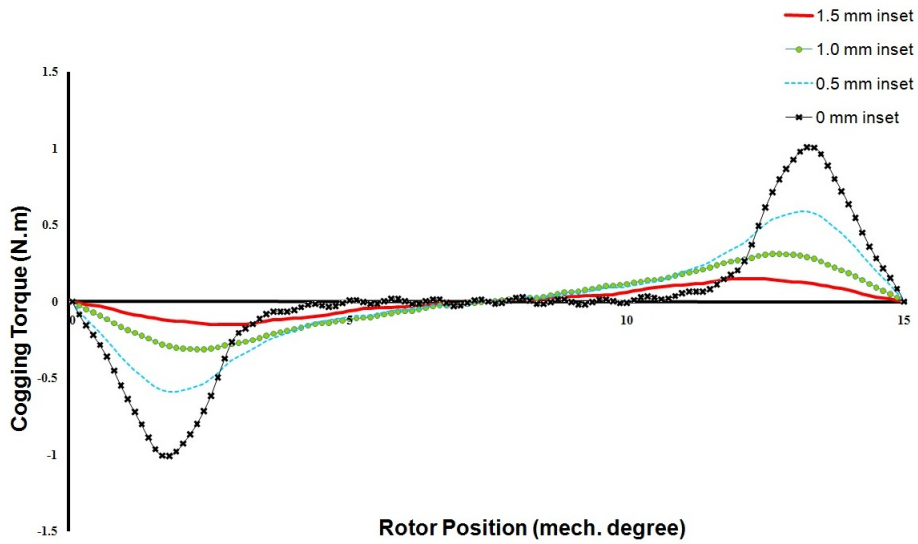


Figure 3.14: Cogging Torque plot for 2.2 kW motor

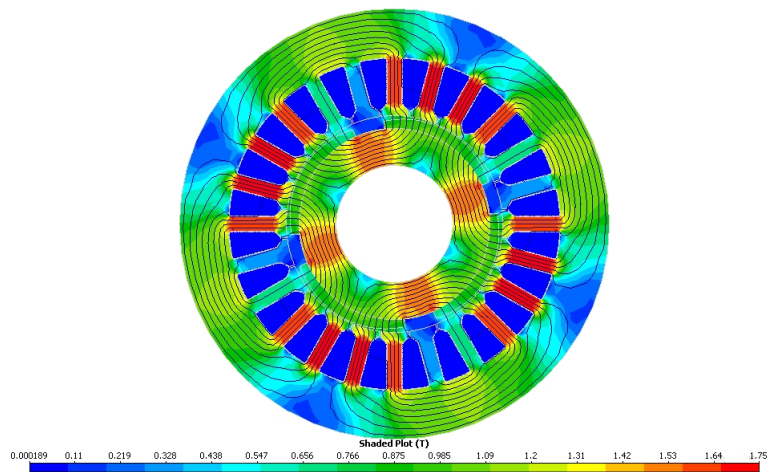


Figure 3.15: Instantaneous field plot of 2.2 kW motor for 1.5 mm magnet edge inset

3. 20 kW Radial flux PMBLDC motor

20 kW radial flux PMBLDC motor is designed based on sizing equations. Computer aided design algorithm is developed for whole design. Model based on design information is prepared and carry out finite element analysis.

Table VII: Reduction in cogging torque by varying magnet edge inset in 20 kW motor

Parameters	Initial design mm	Improved design magnet edge inset in mm		
		0.5	1	1.5
T cog (N.m.)	2.02	1.18	0.628	0.302
T avg (N. m.)	14.4	14.4	14.5	14.5

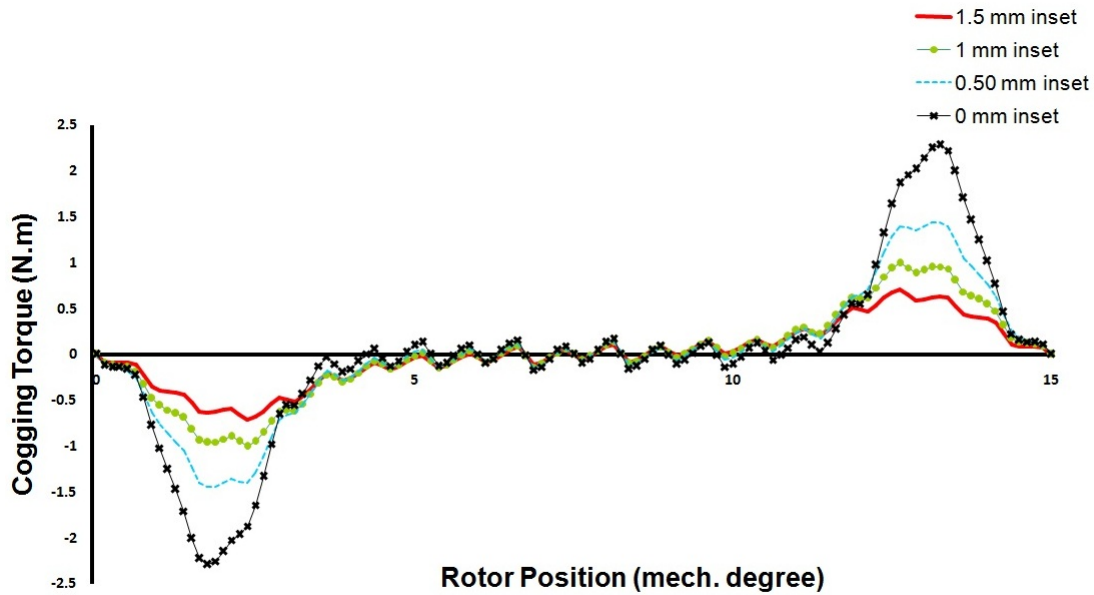


Figure 3.16: Cogging Torque plot for 20 kW motor

Magnet edge inset is varied in improved design by maintaining other design parameters same. Finite element analysis is performed to obtain cogging torque profile. Cogging torque profile is influenced and reduced. It is observed that

peak to peak cogging torque is reduced without affecting other performance indicators. It is observed that flux density in different section of magnetic circuit is as per the assumption.

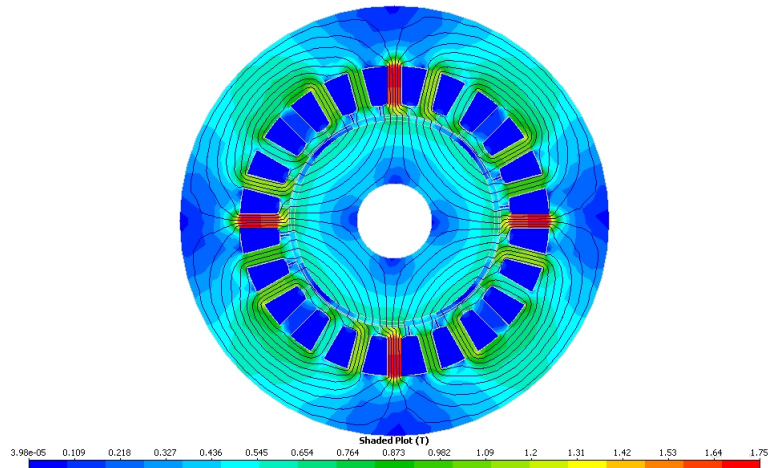


Figure 3.17: Instantaneous field plot of 20 kW motor for 1.5 mm magnet edge inset

3.1.4 Magnet Retaining sleeve

Torque ripple is undesirable component for smooth operation of permanent magnet motors. Cogging torque is prime creator of torque ripple, which creates noise and vibrations. Torque ripple can be lessened by minimizing cogging torque. By proper design improvement in permanent magnet motor, cogging torque can be reduced. cogging torque is minimized in three standard rating motors by selecting proper magnet retention sleeve thickness. Permanent magnets barely bear the high centrifugal force at high speed rotation. The major challenge in high speed permanent magnet motors is to retain magnets properly at high speed. For holding magnet in its place, high strength retention sleeve made of stainless steel is necessary. Initially, motor is designed without magnet retaining sleeve and then after magnet retaining sleeve thickness is varied from 0.1 mm to 0.3 mm. Hence it's concluded that magnet retaining sleeve of permanent magnet motor is effective in cogging torque reduction and its

essential to decide proper thickness of magnet retaining sleeve.

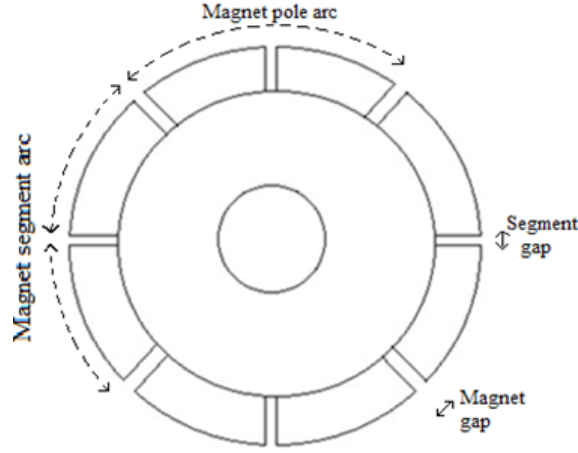


Figure 3.18: PMBLDC motor having 0.3 mm magnet sleeve

1. 70 W Radial flux PMBLDC motor

70 W radial flux PMBLDC motor is designed based on sizing equations. Computer aided design algorithm is developed for whole design. Model based on design information is prepared and carry out finite element analysis.

Table VIII: Cogging torque reduction by varying magnet sleeve in 70 W motor

Parameters	Initial design mm	Improved design magnet retaining sleeve in mm		
		0.1	0.2	0.3
T cog (N.m.)	0.588	0.312	0.272	0.117
T avg (N. m.)	1.91	1.9	1.9	1.9

Magnet sleeve is varied in improved design by maintaining other design parameters same. Finite element analysis is performed to obtain cogging torque profile. Cogging torque profile is influenced and reduced. It is observed that peak to peak cogging torque is reduced without affecting other performance indicators. It is

observed that flux density in different section of magnetic circuit is as per the assumption.

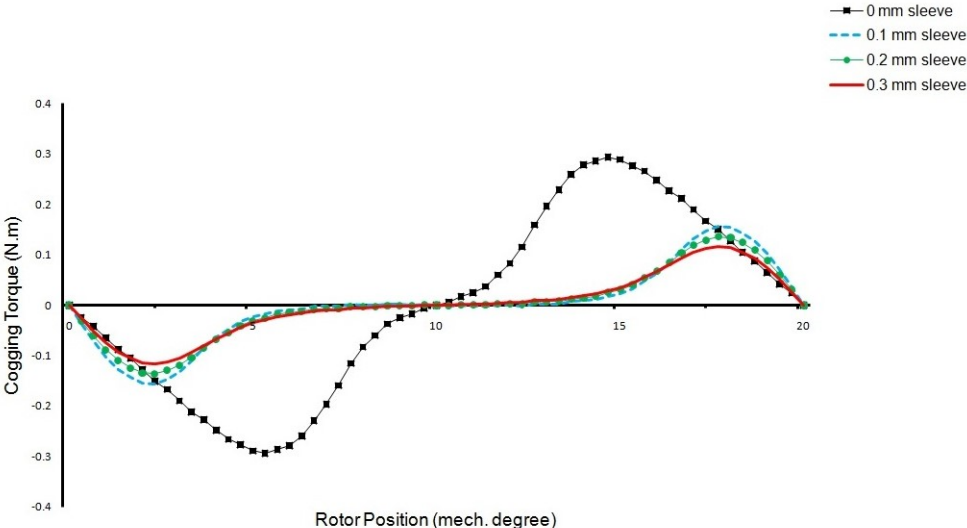


Figure 3.19: Cogging torque profile for 70 W motor

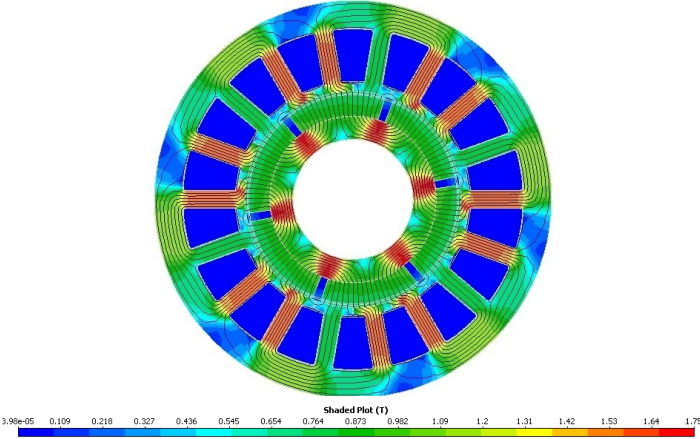


Figure 3.20: Instantaneous field plot of 70 W motor with 0.3 mm magnet sleeve thickness

2. 2.2 kW Radial flux PMBLDC motor

2.2 kW radial flux PMBLDC motor is designed based on sizing equations. Com-

puter aided design algorithm is developed for whole design. Model based on design information is prepared and carry out finite element analysis.

Table IX: Cogging torque reduction by varying magnet sleeve in 2.2 kW motor

Parameters	Initial design mm	Improved design magnet retaining sleeve in mm		
		0.1	0.2	0.3
T cog (N.m.)	10.46	9.46	8.6	7.84
T avg (N. m.)	14.4	14.3	14.3	14.3

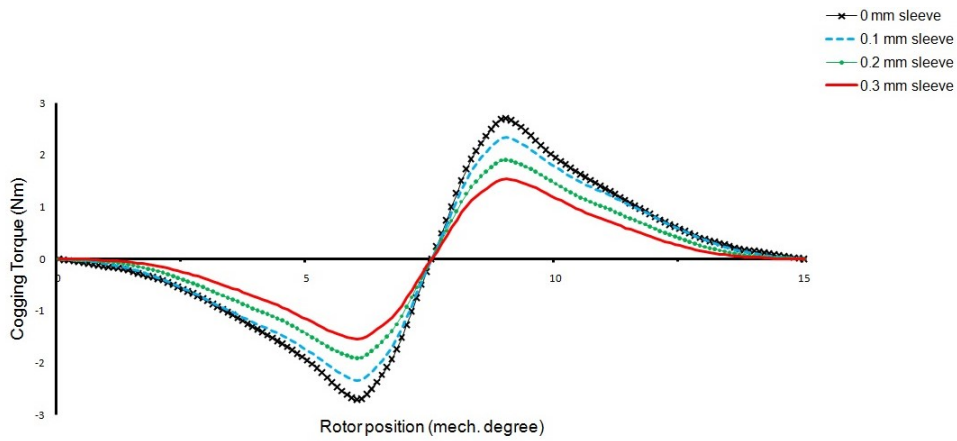


Figure 3.21: Cogging torque plot for 2.2 kW motor

magnet sleeve is varied in improved design by maintaining other design parameters same. Finite Element Analysis (FEA) is performed to obtain cogging torque profile. Cogging torque profile is influenced and reduced. It is observed that peak to peak cogging torque is reduced without affecting other performance indicators. It is observed that flux density in different section of magnetic circuit is as per the assumption.

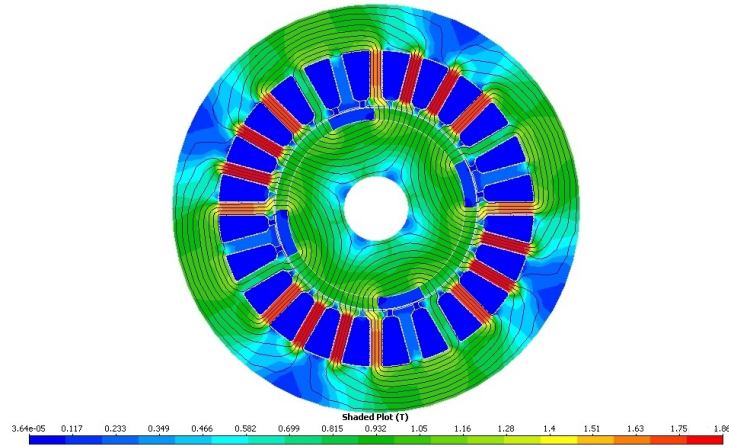


Figure 3.22: Instantaneous field plot of 2.2 kW motor with 0.3 mm magnet sleeve thickness

3. 20 kW Radial flux PMBLDC motor

20 kW radial flux PMBLDC motor is designed based on sizing equations. Computer aided design algorithm is developed for whole design. Model based on design information is prepared and carry out finite element analysis.

Table X: Cogging torque reduction by varying magnet sleeve in 20 kW motor

Parameters	Initial design mm	Improved design magnet retaining sleeve in mm		
		0.1	0.2	0.3
T cog (N.m.)	148.8	139.6	131.6	123.8
T avg (N. m.)	127	126	126	126

Magnet sleeve is varied in improved design by maintaining other design parameters same. Finite element analysis is performed to obtain cogging torque profile. Cogging torque profile is influenced and reduced. It is observed that peak to peak cogging torque is reduced without affecting other performance indicators. It is observed that flux density in different section of magnetic circuit is as per the assumption.

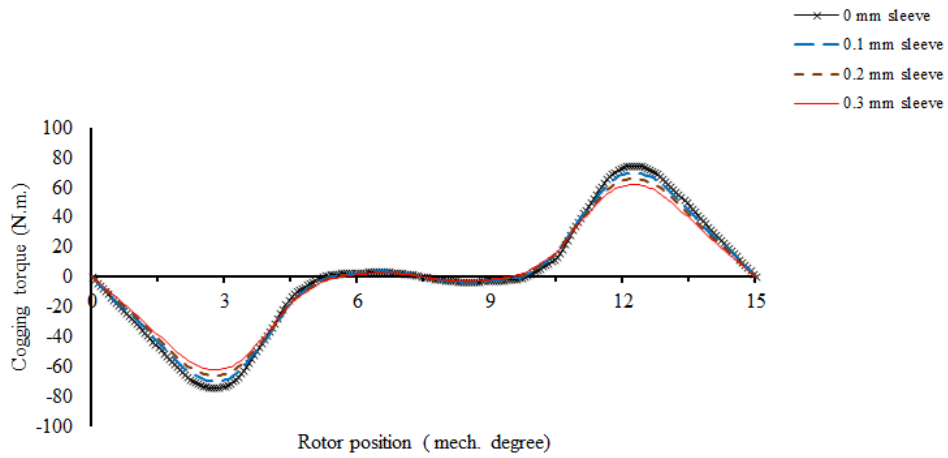


Figure 3.23: Cogging torque plot for 20 kW motor

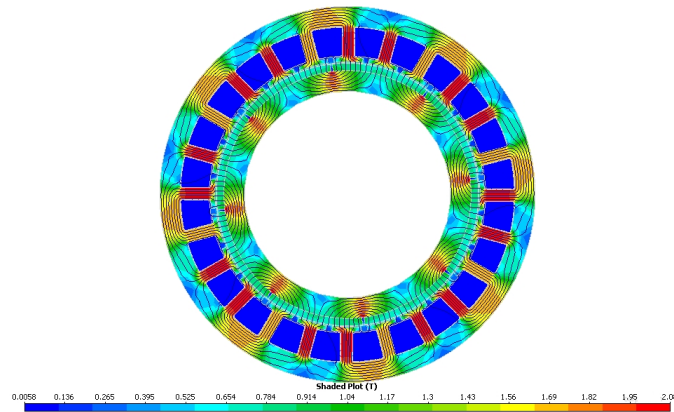


Figure 3.24: Instantaneous field plot of 2.2 kW motor with 0.3 mm magnet sleeve thickness

3.1.5 Stator Slot Depth

Cogging torque is undesirable effect in the brushless dc motor, causing vibration and noise. It arises from permanent magnets interact with the teeth on the stator. By increasing stator slot depth in brushless motor equalize reluctance, reduces cogging torque. 70 W, 2.2 kW and 20 kW motors are analyzed by increasing stator slot depth in order to reduce cogging torque.

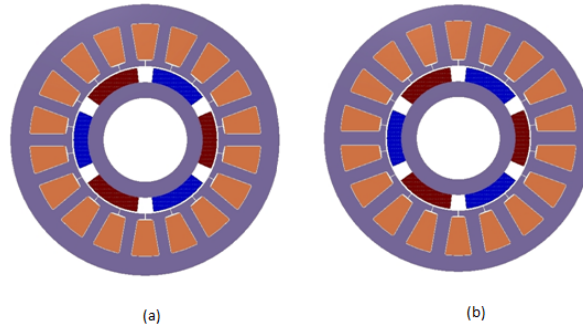


Figure 3.25: (a) Initial design (b) Final design after increment in stator slot depth

1. 70 W Radial flux PMLDC motor

70 W radial flux PMLDC motor is designed based on sizing equations. Computer aided design algorithm is developed for whole design. Model based on design information is prepared and carry out finite element analysis.

Table XI: Cogging torque reduction by varying stator slot depth in 70 W motor

Parameters	Initial design 14.9 mm	Improved design stator slot depth in mm	
		16	16.2
T cog (N.m.)	0.584	.502	0.45
T avg (N. m.)	1.91	1.9	1.91

Stator slot depth is varied in improved design by maintaining other design parameters same. Finite element analysis is performed to obtain cogging torque profile. Cogging torque profile is influenced and reduced. It is observed that peak to peak cogging torque is reduced without affecting other performance indicators. It is observed that flux density in different section of magnetic circuit is as per the assumption.

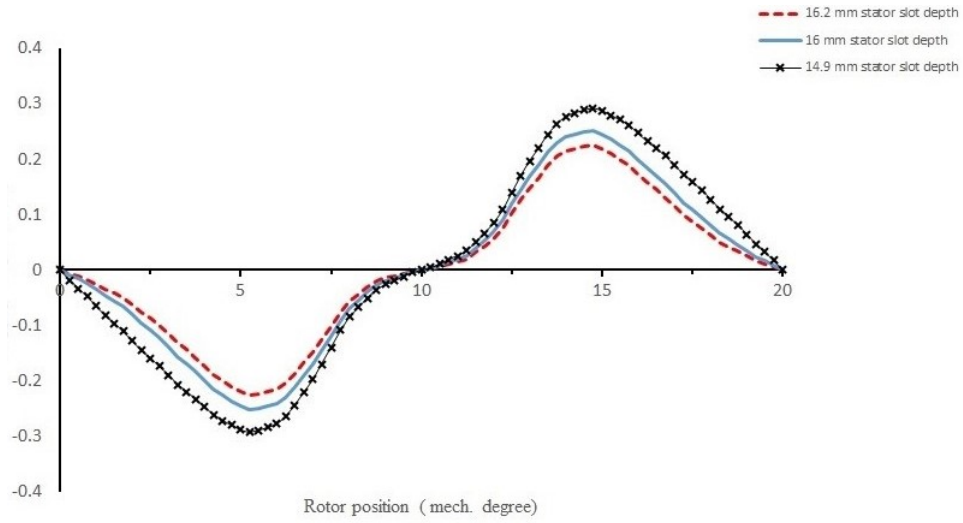


Figure 3.26: Cogging Torque Profile of 70 W motor

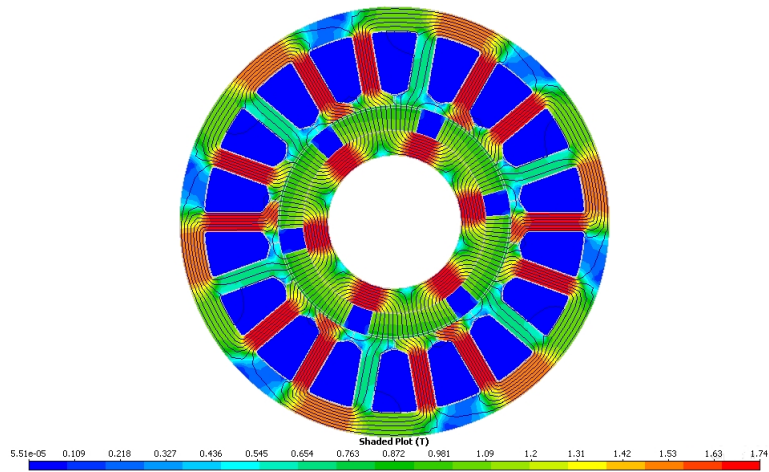


Figure 3.27: Instantaneous field plot of 16.2 mm stator slot depth

2. 2.2 kW Radial flux PMLDC motor

2.2 kW radial flux PMLDC motor is designed based on sizing equations. Computer aided design algorithm is developed for whole design. Model based on design information is prepared and carry out finite element analysis.

Table XII: Cogging torque reduction by varying stator slot depth in 2.2 kW motor

Parameters	Initial design 21.4 mm	Improved design stator slot depth in mm	
		21.9	22.1
T cog (N.m.)	10.32	8.52	7.66
T avg (N. m.)	14.5	14.4	14.4

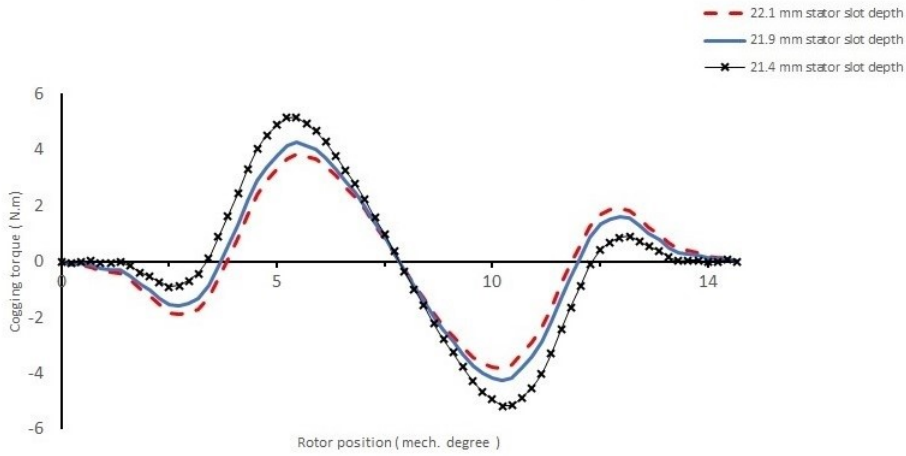


Figure 3.28: Cogging Torque Profile of 2.2 kW model

Stator slot depth is varied in improved design by maintaining other design parameters same. Finite element analysis is performed to obtain cogging torque profile. Cogging torque profile is influenced and reduced. It is observed that peak to peak cogging torque is reduced without affecting other performance indicators. It is observed that flux density in different section of magnetic circuit is as per the assumption.

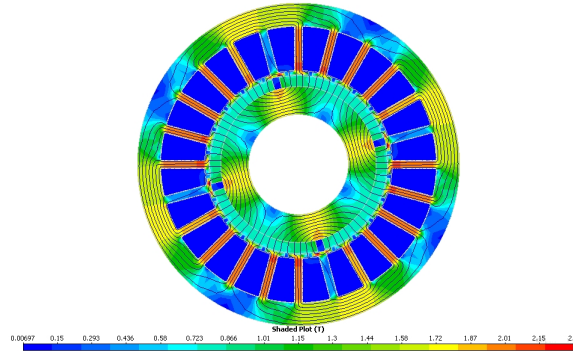


Figure 3.29: Instantaneous field plot of 16.2 mm stator slot depth

3. 20 kW Radial flux PMBLDC motor

20 kW radial flux PMBLDC motor is designed based on sizing equations. Computer aided design algorithm is developed for whole design. Model based on design information is prepared and carry out finite element analysis. Stator

Table XIII: Reduction in cogging torque from initial to improved design in 20 kW motor

Parameters	Initial design 24.4 mm	Improved design stator slot depth in mm	
		25.4	26.3
T cog (N.m.)	48.8	46.6	43.6
T avg (N. m.)	127	127	127

slot depth is varied in improved design by maintaining other design parameters same. Finite element analysis is performed to obtain cogging torque profile. Cogging torque profile is influenced and reduced. It is observed that peak to peak cogging torque is reduced without affecting other performance indicators. It is observed that flux density in different section of magnetic circuit is as per the assumption.

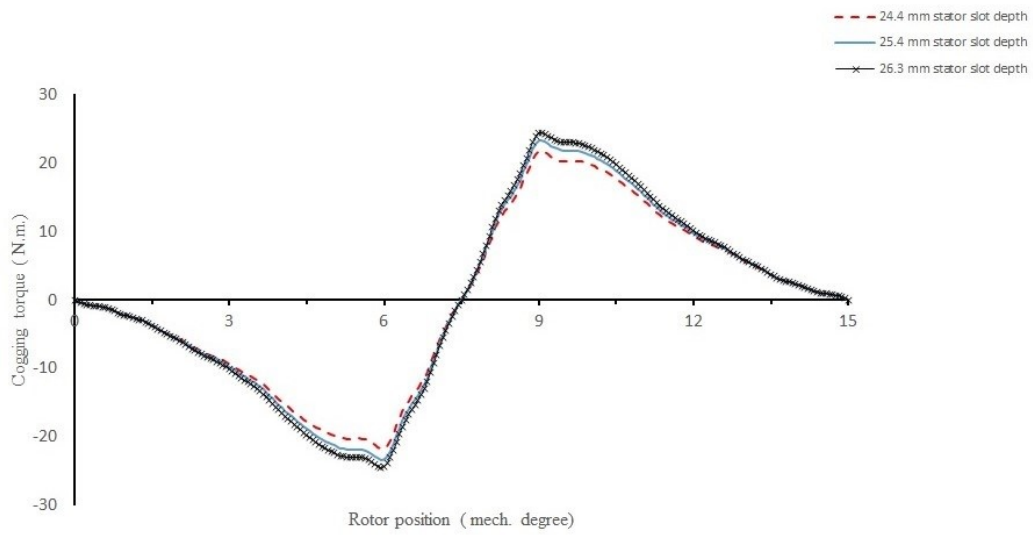


Figure 3.30: Cogging Torque Profile of 20 kW model

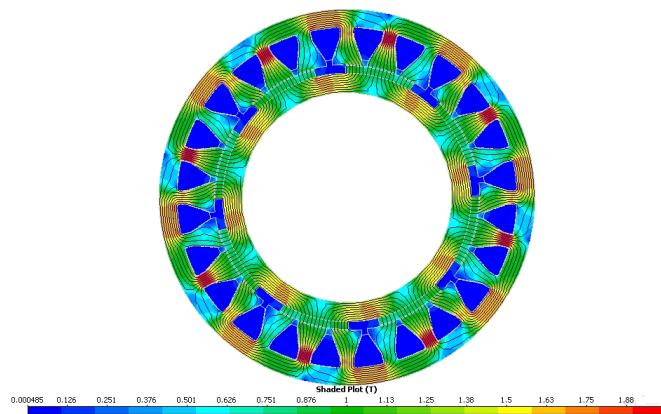


Figure 3.31: Instantaneous field plot of 26.3 mm stator slot depth

3.1.6 Hiperco 50A material

Cogging torque is the one of the drawback of permanent magnet brushless DC motor and prime creator of torque ripple. It's occurs due to interaction between rotor magnet and stator teeth, also known as detent torque because it effects the average torque. The magnetic flux flow from magnets and rotor, and then follows air gap and stator, lastly it returns from the same way. Cogging torque is produce due to variation in reluctance. Reluctance of the air gap is different from the steel which is used in rotor and stator. The cogging torque can be reduced either by making air gap flux zero or the rate of change of the air gap reluctance $dR/d\theta$ to zero. Air gap flux cannot be made zero as a result, cogging torque is lessen by making the air gap reluctance to be constant with respect to rotor position.

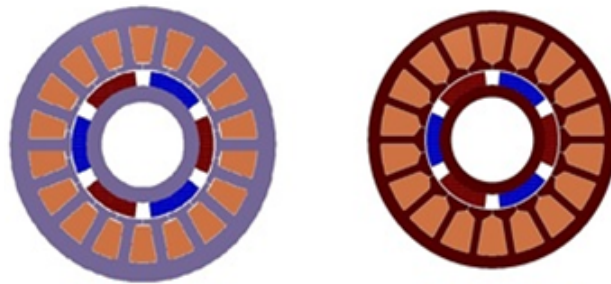


Figure 3.32: Stator and rotor material changed M 19 29 Ga to Hiperco 50A in radial flux PMBLDC motor

1. 70 W Radial flux PMBLDC motor

20 kW radial flux PMBLDC motor is designed based on sizing equations. Computer aided design algorithm is developed for whole design. Model based on design information is prepared and carry out finite element analysis.

Hiperco 50A material is used in stator and rotor by maintaining other design parameters same. Finite element analysis is performed to obtain cogging torque profile. Cogging torque profile is influenced and reduced. It is observed that

Table XIV: Reduction in cogging torque by changing stator and rotor material to hiperco 50A material in 70 W motor

Parameters	Initial design (M 19 material)	Improved design (Hiperco 50A)
Tcog (N.m.)	0.572	0.462
Tavg (N.m.)	1.9	1.91

peak to peak cogging torque is reduced without affecting other performance indicators. It is observed that flux density in different section of magnetic circuit is as per the assumption.

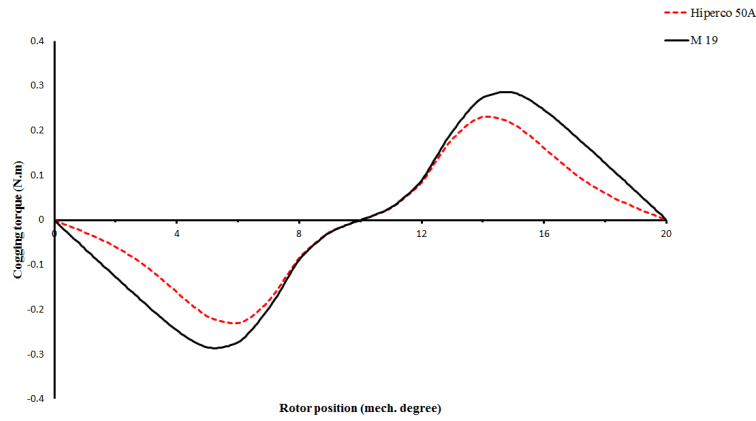


Figure 3.33: Cogging Torque Profile of 70 W model

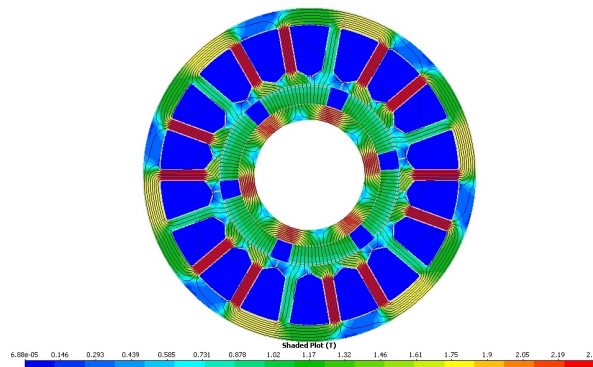


Figure 3.34: Instantaneous field plot of hiperco 50A material of 70 W motor

2. 2.2 kW Radial flux PMBLDC motor

20 kW radial flux PMBLDC motor is designed based on sizing equations. Computer aided design algorithm is developed for whole design. Model based on design information is prepared and carry out finite element analysis.

Table XV: Reduction in cogging torque by changing stator and rotor material to hiperco 50A material in 2.2 kW motor

Parameters	Initial design (M 19 material)	Improved design (Hiperco 50A)
Tcog (N.m.)	10.16	5.62
Tavg (N.m.)	14.4	14.5

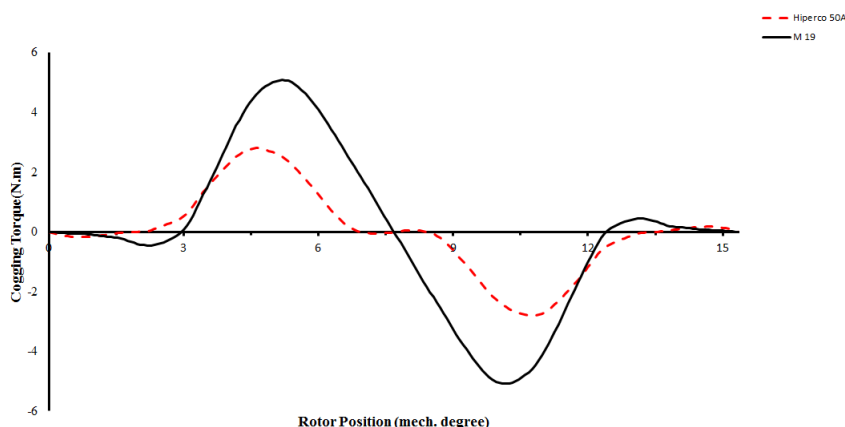


Figure 3.35: Cogging Torque Profile of 2.2 kW model

Hiperco 50A material is used in stator and rotor by maintaining other design parameters same. Finite element analysis is performed to obtain cogging torque profile. Cogging torque profile is influenced and reduced. It is observed that peak to peak cogging torque is reduced without affecting other performance indicators. It is observed that flux density in different section of magnetic circuit is as per the assumption.

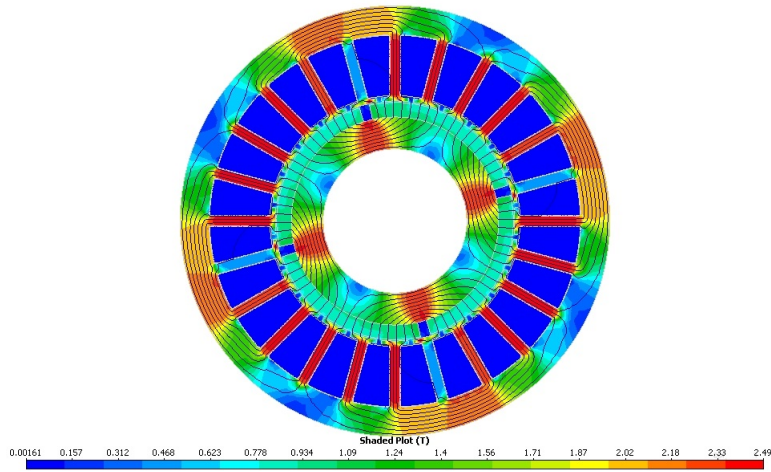


Figure 3.36: Instantaneous field plot of hiperco 50A material of 2.2 kW motor

3. 20 kW Radial flux PMBLDC motor

20 kW radial flux PMBLDC motor is designed based on sizing equations. Computer aided design algorithm is developed for whole design. Model based on design information is prepared and carry out finite element analysis.

Table XVI: Reduction in cogging torque by changing stator and rotor material to hiperco 50A material in 20 kW motor

Parameters	Initial design (M 19 material)	Improved design (Hiperco 50A)
Tcog (N.m.)	48.6	44
Tavg (N.m.)	127	127

Hiperco 50A material is used in stator and rotor by maintaining other design parameters same. Finite element analysis is performed to obtain cogging torque profile. Cogging torque profile is influenced and reduced. It is observed that peak to peak cogging torque is reduced without affecting other performance indicators. It is observed that flux density in different section of magnetic circuit is as per the assumption.

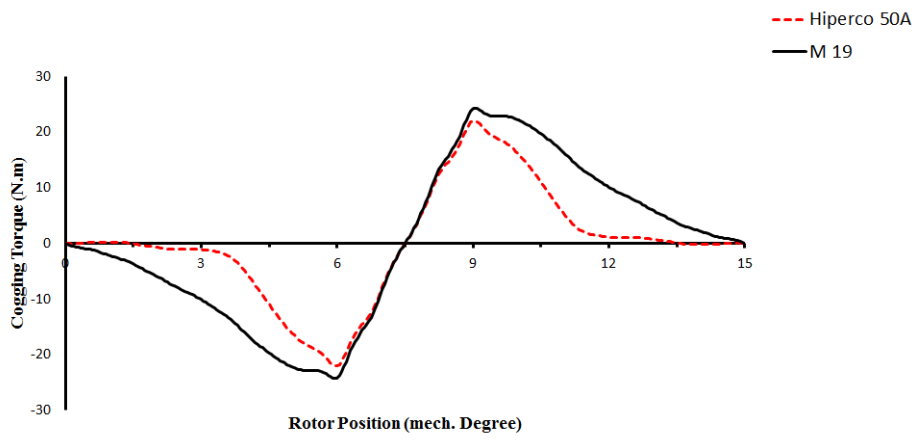


Figure 3.37: Cogging Torque Profile of 20 kW motor

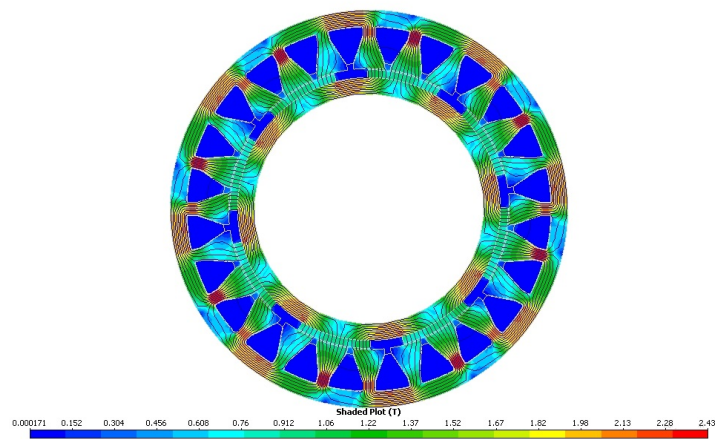


Figure 3.38: Instantaneous field plot of Hiperco 50A material of 20 kW model

Chapter 4

Conclusion and Future work

4.1 Conclusion

Design is done based on basis of CAD output and validation has been done by finite element analysis. Various cogging torque reduction techniques are analyze and then it is observed that tooth tang radius, magnet segmentation, magnet edge inset, magnet retaining sleeve, stator slot depth and hiperco50A material techniques are effective.

4.2 Future work

Detailed analysis of cogging torque minimization techniques can be done to get more accurate results. Also new techniques can be adopted in order to have a better quality of torque and superior performance of the motor. Design of Radial Flux Permanent Magnet Brushless DC Motor with

- Less torque ripple
- Improved efficiency

References

- [1] D.C Hanselman, "*Brushless Permanent Magnet Motor Design*" McGraw hill, New York, 1994.
- [2] J.R Handershoot and T.J.E Miller, "*Design of Brushless Permanent Magnet Motors*" Oxford, U.K., 1994.
- [3] Parag R. Upadhyay and K. R. Rajagopal, "*FE Analysis and CAD of Radial Flux Surface mounted Permanent Magnet Brushless Dc Motors*" published in IEEE transactions on magnetics, vol. 42, no.10, october 2006.
- [4] Chun-Yu Hsiao , Sheng-Nian Yeh and Jonq-Chin Hwang, "*A Novel Cogging Torque Simulation Method for Permanent-Magnet Synchronous Machines*" article ISSN 1996-1073 in 2011.
- [5] Teeradej Srisiriwanna and Mongkol Konghirun, "*A Study of Cogging Torque Reduction Methods in Brushless DC Motor*" published in ECTI transactions on electrical eng., electronics and communications vol. 10,no.2 august 2012.
- [6] Oleg Kudrjajtsev and Aleksander Kilk, "*Cogging Torque Reduction Methods*"
- [7] K. Abbaszadeh, F. Rezaee Alam and M. Teshnehlab , "*Slot opening optimization of surface mounted permanent magnet motor for cogging torque reduction*" published in IEEE Energy Conversion and Management 55 (2012) .
- [8] Prof.Amit N Patel, Malay A Bhavsar and Parth N Patel, "*Sizing of Radial Flux Permanent Magnet Brushless DC Motor*" published in International Conference on Advances in Engineering and Technology 2013, Lovavala
- [9] P. R. Upadhyaya! and K. R. Rajagopal, "*Comparison of performance of the axial-field and radial field permanent magnet brushless direct current motors using computer aided design and finite element methods*" published in journal of applied physics 97,published online 17 may 2005.
- [10] Lei Yan, Ling Luo, Bing Luo and Xianyu Wu, "*Influence of Sleeve on Rotor Eddy Current Loss in 10kW Permanent Magnet BLDC Motors*" published in 17th International Conference on Electrical Machines and Systems (ICEMS),Oct. 22-25, 2014, Hangzhou, China.

- [11] Fengzheng Zhou, Jianxin Shen, Weizhong Fei and Ruiguang Lin, "*Study of Retaining Sleeve and Conductive Shield and Their Influence on Rotor Loss in High-Speed PM BLDC Motors*" published in IEEE transactions on magnetics, vol. 42, no. 10, october 2006 .
- [12] "*Hiperco 50 and hiperco 50A soft magnetic alloys*" in efi ED fagan inc.

Appendix A

Introduction to Motor solve

For accurate designing and finite element analysis of Brushless DC Motor, Induction Motor and Switch Reluctance Motor motorsolve is one of the most advisable software. The output of CAD programme is the input for Motorsolve. Motorsolve input data is supply voltage, speed, rated current, stator outer diameter, length of air gap, length of motor, number of poles, number of stator slot, number of phases, skew angle of rotor, number of magnet per pole, rotor yoke width, rotor inner diameter, stator inner diameter, magnet arc angle, magnet thickness, stator yoke width, rotor outer diameter, conductor slot depth, conductor cross sectional area, total slot depth, shoe depth, slot opening, number of stator slot per pole per phase, width of teeth, SWG number, coil span, number of layers, number of turns per coils in single layer, number of turns per coils in double layer, stacking factor etc.

Main Features of MotorSolve

Motor type : Brushless DC machine(BLDC) , Induction machine(IM), Switched Reluctance machine(SRM) are supported.

Sizing : Allow one to quickly establish the preliminary dimension of motor design based on the output requirement and supply voltage.

Template-based variational geometry engine : Includes dozens of editable rotor and stator types that allow one to quickly create the required motor configuration.

Automatic stator winding Layout : Computes the possible balanced winding layouts, which can be edited by the user.

Materials : MotorSolve includes an extensive database of steels and permanent magnet material.

Results : Provided as waveforms, charts and field plots allowing one to quickly assess the device's performance.

Methods of FE analysis are :

There are four methods for result analysis

- Motion Analysis
- Pwm Analysis
- D-Q Analysis
- Lumped parameters

Motion Analysis : It generates a chart of performance result as a function of time. The motor is driven by an ideal current source. Motion analysis is more accurate

than PWM analysis.

PWM Analysis : User can see the effect of switching on the performance of the motor. This method does not take the sleeve or magnet eddy-current losses into account.

D-Q Analysis : This is the fastest analysis among all. This analysis generates a chart of performance results as a function of current, advance angle, and /or speed. The results are calculated from the d-q model of motor, which is updated for each current and advance angle.

Lumped parameters : This is useful for generating values that can be used in an equivalent circuit model. It generates a chart of selected lumped parameter result quantities. The results are calculated from the d-q model of motor, which is updated for each current and advance angle.

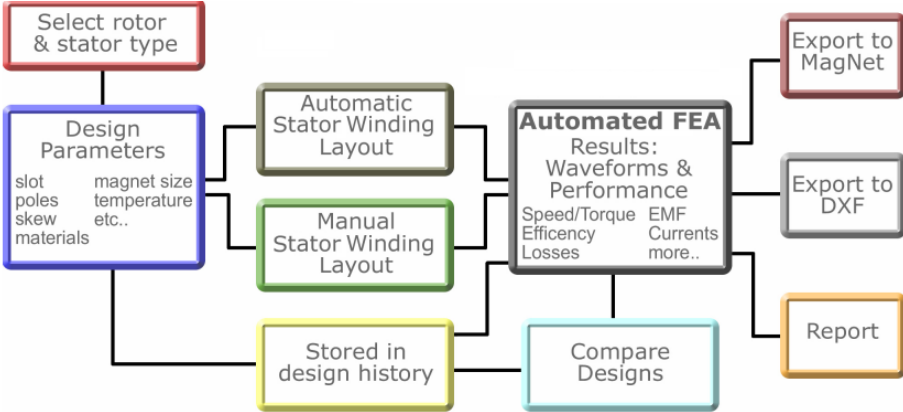


Figure A.1: Motor solve work flow

Appendix B

List of Publication

1. Amit N. Patel, Amit Kapil, Analysis of Cogging Torque Reduction by Increasing Stator Slot Depth in Brushless DC Motor, International Journal of Research and Scientific Innovation (IJRSI) held on 24th December 2015 at Gujarat.

2. Amit N. Patel, Amit kapil Effect of Magnet Retaining Sleeve Thickness on Cogging Torque of Radial Flux Permanent Magnet Brushless DC Motor, International Electronic and Electrical Engineering (IEEE) held on 24th - 26th February 2016 at thanjavur, Tamil nadu.